the ISBA land-surface scheme has been assessed. The topology of the cost function has been studied using simulated observations. The uncertainty in the distribution of water between the two surface reservoirs and the influence of various parameters (water stress, fraction of vegetation, solar radiation intensity, frequency of 2m observations, length of the assimilation period) on the quality of the analyzed surface fields have been evaluated. The covariances of background errors used both for the optimal interpolation and the variational surface analyses were estimated on the experimental site MUREX with a direct method (using observations) and a Monte-Carlo one. These two analysis schemes have been tested over a full annual cycle with simulated and real observations. It has been useful to define different assimilation windows according to the associated time scales of the analyzed surface fields in the variational analysis. This method gave better results than the optimal interpolation because of the temporal consistency of the observations on the assimilation period for the total water content analysis and the assimilation of asynoptic observations for the fields with short time scales evolutions. Both methods are however very sensitive to the presence of 2m biases which are not caused by surface errors, pointing out the importance of the model quality in terms of radiative and hydrological forcings.

Doctor Luc GERARD

Physical parameterisations for a high resolution operational numerical weather prediction model

Summary of PhD presented at Brussels Free University on August 31, 2001 for the doctorate in Applied Sciences

In a first part, we provide an up-to-date description of the whole set of physical parameterisations used in the operational Aladin model (this part is also published separately as the documentation of Aladin Physics, available on the web site).

We focus then on the present parameterisation of deep convection. Our personal contribution to this concerned the entrainment of horizontal momentum into the convective cloud. We then discuss the main weak points and the hypotheses of the scheme that would need revisiting in order to reduce the mesh sizes, and propose paths to new developments.

We assess more deeply two proposals emerged from this discussion: using prognostic variables for convective activity, and introducing a distinction between the properties of the air at the immediate cloud vicinity (‘‘environment’’, which is the air entrained into the cloud) and the value of the resolved model fields.

This leads to the development of a prognostic scheme for the up- and downdraught vertical velocities and active mesh fractions. Such a scheme should still be complemented by a prognostic parameterisation of the suspended condensate (still in development by others) and a few other enhancements that we propose.

The implementation of the prognostic scheme includes the advection by the resolved wind of the 4 new prognostic variables, performed in grid point only. Further tests confirmed that no coupling was necessary for such prognostic internal variables.

A first set of tunings of the scheme was performed in Single Column Model. This showed for instance that shortening the time step (similar to reducing the mesh size in a 3D model) induces a progressive extinction of the prognostic scheme, while the diagnostic scheme proceeds by abrupt cuts (following the feedback of the resolved precipitation) of its activity.

Validation and behaviour tests were performed in Local Area Model (ALADIN) at two different resolutions and in Global Circulation Model (ARPEGE) at four different truncations.

Behaviour tests yielded a spin-up time of about half an hour, consistent with observations of convective systems. The convergence of the prognostic scheme with the diagnostic scheme for very large time steps was tested by lengthening artificially the physical time step in the convection routine, for both schemes. We observed a good convergence when multiplying the time step by 30, which alerted us that the convergence of the results was not be expected with the present truncations used in the GCM. The tests in GCM at different truncations showed indeed always different behaviours with the diagnostic and the prognostic scheme.

The more progressive start of the prognostic scheme leads to a slower development of the convective activity than with the diagnostic scheme. To compensate this, it helped reducing the entrainment coefficients (which modulate the cloud activity), but we think a wider re-tuning would be welcome.

The impact of the new scheme on the global budgets has also been approached. Zonal diagnostics suggest a possible enhancement by the prognostic approach, of the temperature and water vapour mean tendencies; but more systematic tests should be done after a complete tuning.

The experiments brought new insights in the behaviour of the convective scheme and on the problem of merging contributions from the subgrid deep convection scheme and the resolved precipitation scheme. The use of meshes thinner than 5 km requires to leave the hydrostatic approximation in the large scale equations, and we envisage potential refinements of the parameterisation in this case.

ALADIN PhD Studies

1. Radi AJJAJI : "Incremental deficiencies in ARPEGE 4D-Var assimilation system"

As it was discussed in the last ALADIN Newsletter, a number of experiments made with the ARPEGE 4d-var system, to diagnose the problem of the appearance of large positive humidity increments over some subtropical land areas, were performed. They didn't reveal any interesting result. They were, for most of them, rerun because of a dirty error in the 4d-var chain scripts used. But again without any new result. For remember these experiments were carried out to study :

- the impact of simplified physics,
- the impact of a "multiple truncations" incremental approach,
- the impact of a "unique truncation" incremental approach,
- the impact of Full-Pos on the increments,
- ... etc.

The overestimated precipitations (linked to this large positive humidity analysis increments) observed on Sahara region, are also present over the USA in June/July period, and on other subtropical hot regions. It has been shown that these large short-range forecast errors exist in ARPEGE but not in other models as the ECMWF or UKMO ones.

Thanks to François Bouttier, sensitivity experiments, executed with no specific humidity in the cost function, revealed the presence of a non-zero gradient with respect to the specific humidity parameter. So it turns out that there is something annoying in the TL/AD formulation of the dynamics. The specific humidity increments are caused by the linearization of three terms in the dynamics :

$$C_p = q\, C_{pv} + (1-q)\, C_{pd}$$

$$R = q\, R_v + (1-q)\, R_d$$

$$d(RT) = T\, dR + R\, dT$$

This three terms are coded respectively in GPRCP, GPRCP and CPG. *d(.)* indicates the Lagrangian derivative. Indices *v* and *d* stand for "dry" and "vapour" respectively.

Experiments done by F. Bouttier revealed also that more than 90% of the humidity increments are caused by the adjoint of the third above equation.

This fact happens, for example, in Sahara region because, apparently, there is a combination of high temperatures and large horizontal gradients of *(RT)* on the model surfaces. One must keep in mind that this is not due to incorrect adjoint formulation, it is a feature of the dynamics equations. It seems that a solution of the problem could be the introduction of some extra terms into the TL/AD models, to prevent large local derivatives. The problem is probably not limited to the humidity field.

As a first confirmation of this investigation, an experiment consisting in forcing R_v by R_d along the 4d-var minimisation, is performed.

$$d(RT) = (R_v - R_d)\, T\, dq + ...$$

$$d(grad\, q) = (R_v - R_d)\, T\, d(gradT)$$

As it can be seen on the figures below, the problem disappears completely. But putting :

$$R_v = R_d$$

is not the solution of the problem, it is just a mean to confirm the importance of local derivatives in the TL/AD part. More investigations need still be done to find a scientific reasonable cure.

From figures, one can notice that, when compared to 3d-var, the experiment with R_v forced to R_d is the better one, indicating that the formulations of the TL/AD of dynamics still need some tuning to work correctly.

Figure 1 : Convective precipitations (00+24H) over Sahara area, for the period between 01/06/2000 and 10/06/2000. Right column : operational charts. Left column : 3d-var reference charts. Middle column : results when forcing R_v to R_d in 4d-var.

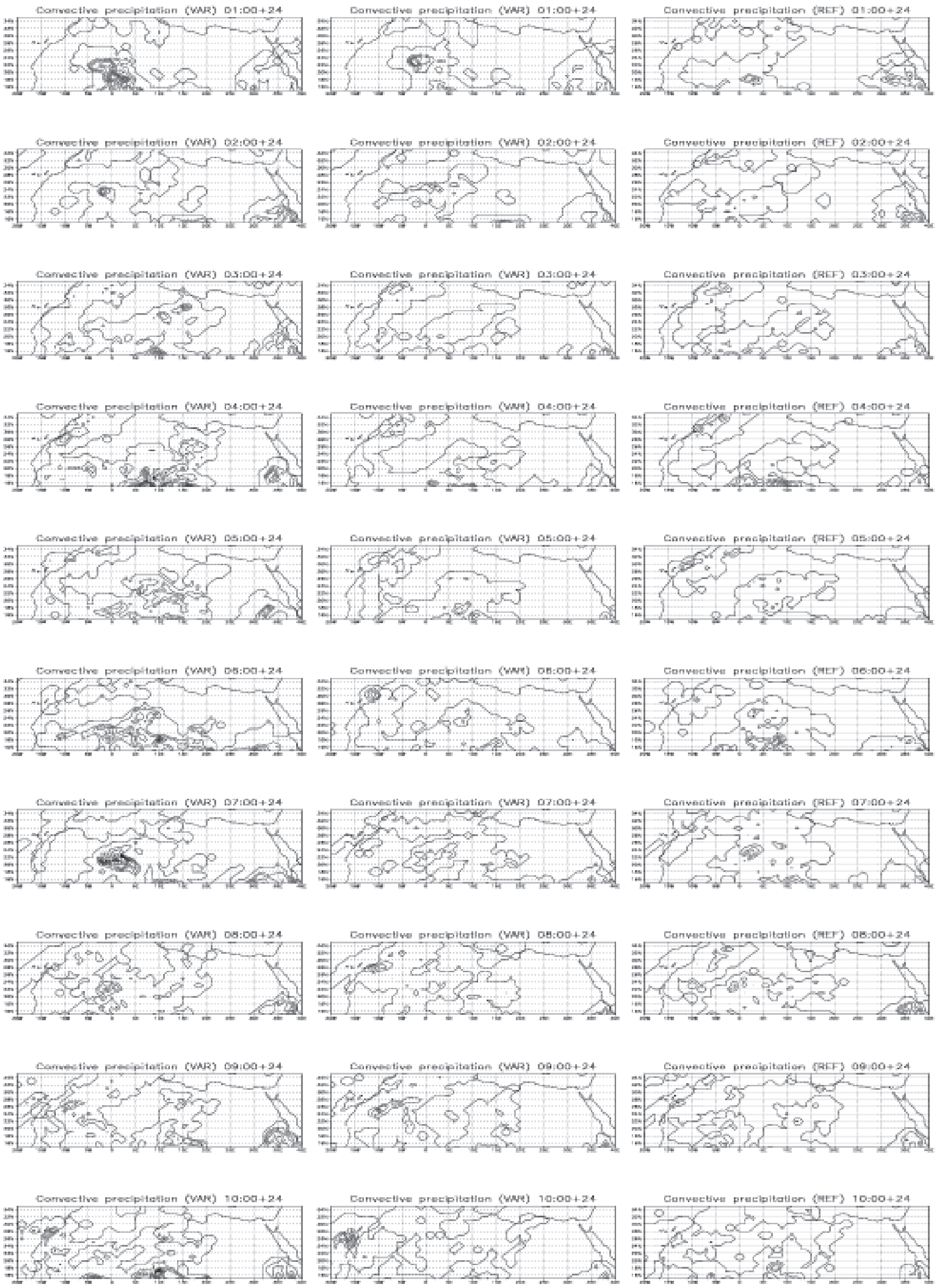

Figure 2 : Zonal means of specific humidity (right), relative humidity (middle) and temperature (left). From top to bottom : operational 4d-var against 3d-var, adiabatic 4d-var against 3d-var, unique truncation incremental 4d-var against 3d-var, experiment $R_v = R_d$ against 3d-var.

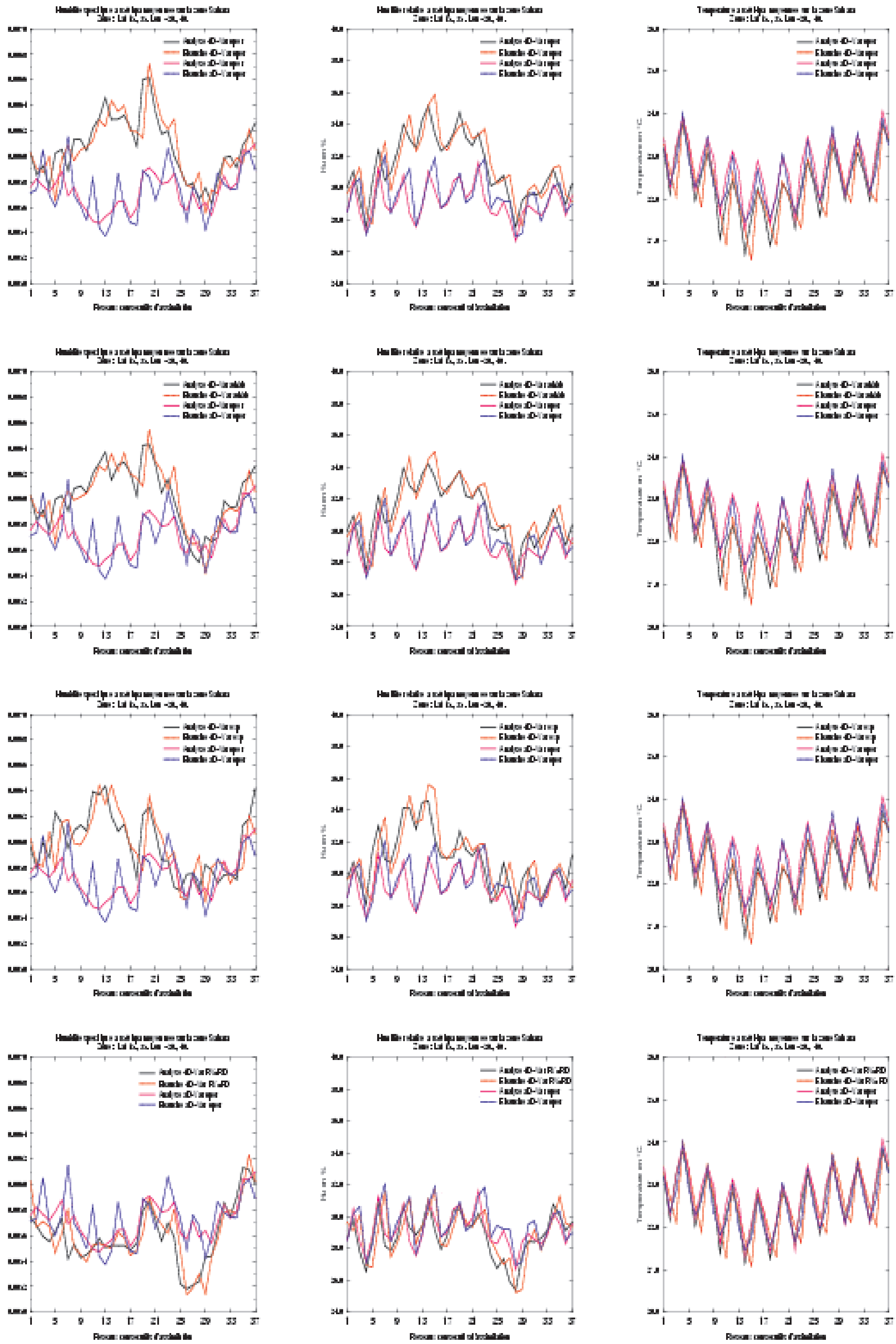

Figure 3 : Same as figure 2, but for zonal means averaged on standard levels over a 10-days assimilation experiment.

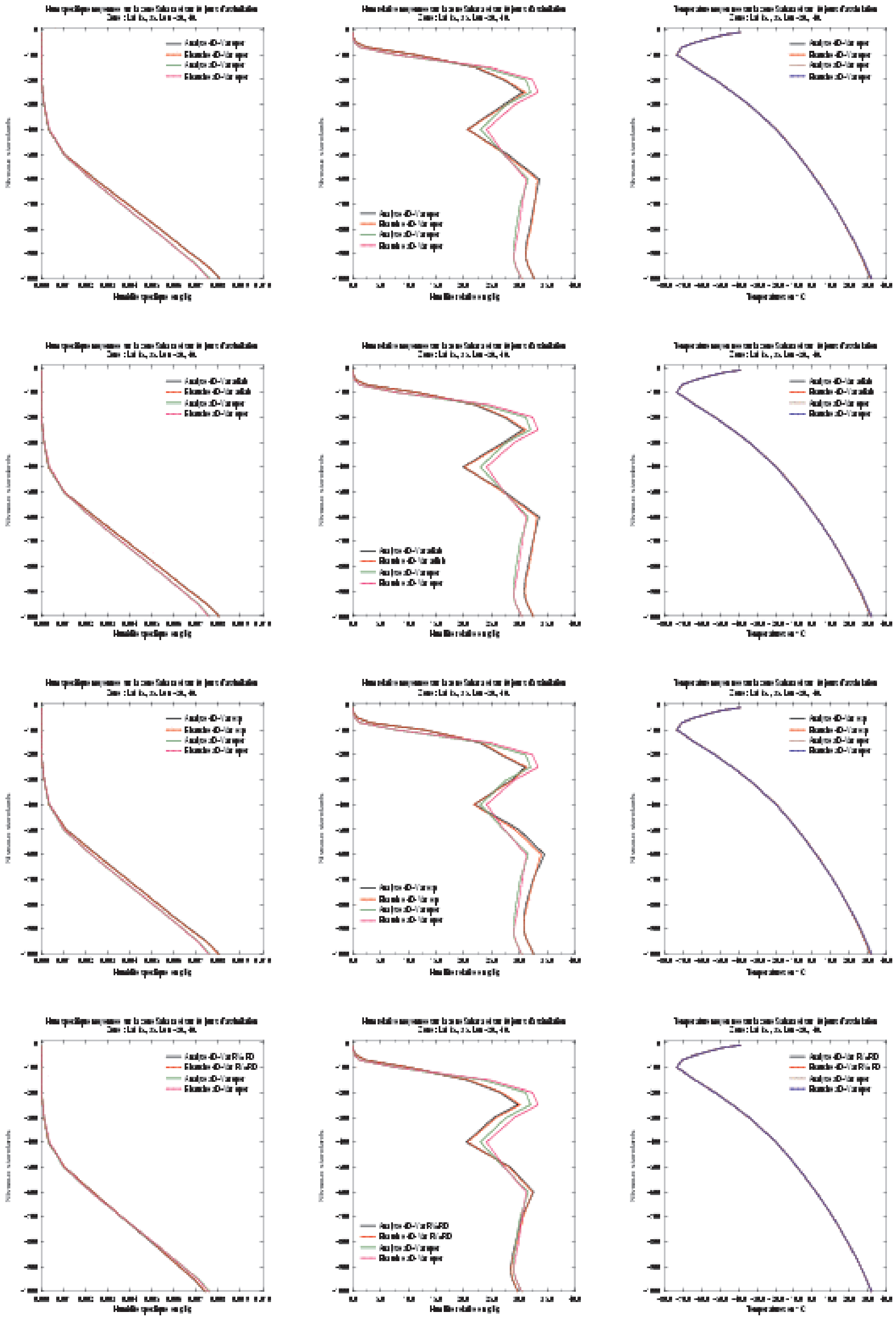

2. Jean-Marcel PIRIOU : "Correction of compensating errors in physical packages ; validation with special emphasis on cloudiness representation"

See :"*Ways to address the issue of compensating errors in physical parameterization*s" by Jean-Marcel Piriou in the proceedings of the 10th ALADIN workshop and the ALADIN & ALATNET reports for Toulouse in this Newsletter.

3. Wafaa SADIKI : "A posteriori verification of analysis and assimilation algorithms and study of the statistical properties of the adjoint solutions

Last news in Newsletter 19.

4. Filip VANA : "The dynamical and physical control of kinetic energy spectra in a NWP spectral semi-Lagrangian model"

Last news in Newsletter 19.

ALATNET PhD and Post-Doc Studies

1. Gianpaolo BALSAMO : "Coupling a variational assimilation of gridpoint surface fields with a 4d variational assimilation of upperair spectral fields"

A variational assimilation technique is considered to analyse the soil variables by assimilating 2*m* data of temperature and relative humidity. We consider 2-D (z and t) variational approach, under the assumption of horizontal decoupling of surface processes between grid points. This hypothesis is firstly supposed considering the small scale involved in the soil processes far from the actual grid mesh in NWP (few meters against few km). A validation test is then designed to evaluated the influence of neighbours grid points. Thus, the method is applied on every grid point singularly and the gain matrix is directly computed given the small dimension of the problem. The variational technique keeps count of the full physics of the model and therefore the corrections applied on the control variable are adapted to the current meteorological conditions and the grid point characteristics (texture, vegetation fraction, LAI, ... and the previous soil state). The observation departures are computed at the synoptic time (00 06 12 18 UTC) and a linear estimation of observation operator is obtained by applying a perturbation to the control variable (W_s, T_s, W_p, T_p). A first test on a 48 h time window for the total soil moisture content (W_p) analysis is presented. A sequential assimilation cycle every 6h is also studied as it allows to focus on specific problems.

The linearized variational approach

The assimilation of the data in NWP consists in best fit the data and the model previous information. This optimal state is obtained by the minimization of the cost function J(x), of the form:

$$J(\mathrm{x}) = J^{b}(\mathrm{x}) + J^{o}(\mathrm{x}) = ½\,(\mathrm{x} - \mathrm{x}^{b})^{T}\,\mathbf{B}^{-1}\,(\mathrm{x} - \mathrm{x}^{b}) + ½\,(\mathrm{y} - H(\mathrm{x}))^{T}\,\mathbf{R}^{-1}\,(\mathrm{y} - H(\mathrm{x})) \qquad (1)$$

where:

x is the control variables vector $(\mathrm{x} = (\mathrm{x_i})_{1 \leq \iota \leq n})$

x^{b} is the control variables vector $(\mathrm{x}^{b} = (\mathrm{x_i}^{b})_{1 \leq \iota \leq n})$

y is the observation vector $(\mathrm{y} = (\mathrm{y_i})_{1 \leq \iota \leq n})$

H is the observation operator, $\mathbf{H}$ its linear approximation

x^{t} is the real state, $\mathrm{y}^{t} = H(\mathrm{x}^{t})$

$\mathbf{B}$ is the matrix of forecast errors covariances

$\mathbf{R}$ is the matrix of observation errors covariances

$$\mathbf{B} = \overline{(x_i - x_i^{t})(x_j - x_j^{t})^{T}}_{1 \leq i,\, j \leq n} \qquad \mathbf{R} = \overline{(y_i - y_i^{t})(y_j - y_j^{t})^{T}}_{1 \leq i,\, j \leq p}$$

The observation operator H transports the state vector x into the observations space. This includes geometrical and physical interpolation as well as integration in time. This method needs normally an effort of coding the tangent linear and the adjoint of the direct code of the model in order to perform the minimization of the cost function. For low dimension problems, the minimization of the cost function can be imposed directly by the expression:

$$\nabla_{\mathrm{x}}\, J(\mathrm{x}) = 0 = \mathbf{B}^{-1}\,(\mathrm{x} - \mathrm{x}^{b}) + \mathbf{H}^{T}\,\mathbf{R}^{-1}\,(\mathrm{y} - H(\mathrm{x})) \qquad (2)$$

When this condition is satisfied $\mathrm{x} = \mathrm{x}^{a}$. The H operator can be expressed by the Taylor prime order expansion under the linear hypothesis:

$$H(\mathrm{x}+\delta\mathrm{x}) = H(\mathrm{x}) + \mathbf{H}\delta\mathrm{x} \qquad (3)$$

By substituting the expression (3) in the equation (2) and rearranging it, is obtained:

$$\nabla_{\mathrm{x}}\, J(\mathrm{x}^{a}) = 0 = \mathbf{B}^{-1}\,(\mathrm{x}^{a} - \mathrm{x}^{b}) + \mathbf{H}^{T}\,\mathbf{R}^{-1}\,(\mathrm{y} - H(\mathrm{x}^{b}) - \mathbf{H}(\mathrm{x}^{a} - \mathrm{x}^{b})) \qquad (4)$$

$$\mathrm{x}^{a} = \mathrm{x}^{b} + \mathbf{BH}^{T}(\mathbf{HBH}^{T} + \mathbf{R})^{-1}(\mathrm{y} - H(\mathrm{x}^{b})) \qquad (5)$$

where the terms:

$$\mathbf{K} = \mathbf{BH}^{T}(\mathbf{HBH}^{T} + \mathbf{R})^{-1} \qquad \mathrm{y} - H(\mathrm{x}^{b}) \qquad (6)$$

are respectively the gain matrix $\mathbf{K}$ and the innovation vector. This equation recalls the formulation of the Best Linear Unbiased Estimate (BLUE) but including the integration in time. The method requires an extra integration of the model initialised with a perturbed state of the control soil variable to analyse. The perturbation provides a linear estimation of the Jacobian of the observation operator H. The linear hypothesis is best satisfied in the vicinity of x^{b}, so the method is suitable to be applied for small correction of the first guess.

Application of the method for W_p analysis

The analysis of total soil water content W_p of the ISBA scheme using 2*m* observations (temperature *T* and relative humidity *Hu*) is presented as an example. Considering the 2*m* variations between the guess *G* and its perturbation *G'*:

$$\delta T_{2m} = T_{2m}^{G'} - T_{2m}^{G} \qquad \delta Hu_{2m} = Hu_{2m}^{G'} - Hu_{2m}^{G} \tag{7}$$

The matrices **B**, **R**, **H**, used for the direct computation of **K** are simply:

$$\mathbf{B} = \left(\sigma_{W_p}^2\right) \qquad \mathbf{R} = \begin{pmatrix} \sigma_{T_{2m}}^2 & 0 \\ 0 & \sigma_{H_{2m}}^2 \end{pmatrix} \qquad \mathbf{H} = \begin{vmatrix} \frac{\delta T_{2m}^{(1)}}{\delta W_p} \\ \frac{\delta Hu_{2m}^{(1)}}{\delta W_p} \\ \ldots \\ \frac{\delta T_{2m}^{(N)}}{\delta W_p} \\ \frac{\delta Hu_{2m}^{(N)}}{\delta W_p} \end{vmatrix}$$

The innovation vector is given by the difference between the observation and the reference at the grid point for T_{2m} and Hu_{2m}. Here no approximation is required, but the difference is performed at the grid point instead of the observation point. This practically implies a previously analysed field for T_{2m} and Hu_{2m}. The form of the innovation vector is as follows:

$$\mathrm{y} - H(\mathrm{x}^b) = \left(\Delta T_{2m}^{(1)} \quad \Delta Hu_{2m}^{(1)} \quad \ldots \quad \Delta T_{2m}^{(N)} \quad \Delta Hu_{2m}^{(N)} \right)$$

The experimental frame to test the convergence

To investigate the general convergence of the method, several experiments are performed. A model run initialised with a well known reference state of soil moisture W_{ref} is used to extract simulated observations (OBS=GUESS of the reference run). The error of the analysis is evaluated as:

$$Err(W_p^a) = W_{ref} - W_{analysis} \tag{8}$$

The accuracy of the method to retrieve an error equal to the perturbation applied is fair. For a perturbation of $\delta W_p = 10$ mm applied on each grid point, the use of simulated observations allows to retrieve a correction of 10 mm with a mean absolute error lower than 5.2 10^{-6} *mm*. The accuracy is dependent on the error covariances assumed for the background and the observation terms. Therefore to have a greater convergence towards the simulated observations, the standard deviations (σ) for observational errors are chosen of low magnitude (0.01 *K* for T_{2m} and 0.1 % for Hu_{2m}), and that for background (W_p) is put to 100 *mm*. A set of randomly generated state of W_p with given mean and standard deviation is now considered as first guess. From the different departures (W1, W2, W3 for wet guess, D1, D2, D3 for dry guess) generated with a linear random distribution around a given mean value it is checked the convergence towards the reference (W_{ref}).

The perturbation *G'* is produced from the guess **G** according to the following condition:

$$W_p^{G'} = \begin{matrix} W_p^G + 0.1 \cdot (W_{fc} - W_{wilt}) & if \;\; W_p^G < W_p^{med} \\ W_p^G - 0.1 \cdot (W_{fc} - W_{wilt}) & if \;\; W_p^G > W_p^{med} \end{matrix} \qquad where \;\; W_p^{med} = (W_{fc} - W_{wilt}) / 2 \tag{9}$$

Coupling files are taken from the 16-17 June 2000 and the observations are generated from the reference run without noise (perfect observations).

Assimilation on 48 hours time window

A 48 hours test from the different departures gives indication of mean convergence. The maps of W_p errors show some patterns of not convergent points over eastern Europe and southern Italy that can be put in relation with the synoptic situation. The main reasons for the poor local convergence can be attributed to the little information content in meteorological perturbed areas or in mountainous regions. Anyway, by iterating the convergence it is reached an equilibrium state (from every W_p departure) where the percentage of total land points that converge with an error lower than 10 *mm* is around 70 % and becomes greater that 94 % if we consider errors lower than 30 *mm*.

A 6h sequential assimilation cycle

Following the results of the 2-D (z and t) variational approach for a long time window, the method has been applied in sequential way with a 6 hour forecast cycle. This allows to better understand the relations with meteorological situation and to see the impact of each network assimilated. The **H** matrix is evaluated considering 6h forecast (at time t) starting from the guess *G* and its perturbation *G'* (initialised with the corresponding values of W_p at the time t-6h). The convergence at the end of the 48 hours period (after 8 cycles) is reached with an error lower than 10 *mm* for 82 % of the points and 96 % if we consider errors lower than 30 *mm*.

Study of the behaviour of the **H** *matrix*

The estimation of **H** matrix by mean of a perturbed forecast could lead to undesired variation of other near-surface or vertically cumulated fields. Particularly the precipitation (as shown in figure 1), the 10*m* wind, and the incoming solar radiation (and also the cloudiness to cover nocturnal hours) are considered. A further test is done to put in evidence the effect of the synoptic situation on 2*m* temperature during the integration. The figure 1 shows the time-step evolution of the guess and the perturbed run for T_{2m} at 2 points located respectively in clear sky and rainy situation. Although the mean behaviour of T_{2m} is similar, with a higher temperature for perturbed guess field, the resulting gradient is of opposite sign due to stronger oscillation in rainy conditions. This leads over certain areas (figure 2 *left*) to a noisy representation of the **H** matrix, which is responsible for the local poor convergence. Those situations are likely to occur when the atmosphere is interested by precipitation events, reduced solar radiation flux (cloudy condition) or strong lateral advection. A set of constraints are applied by masking grid points where the sensitivity to initial conditions (evaluated as difference between the guess and its perturbation *G - G'*) overpass a given threshold. As a result the main noisy patterns shown in figure 2 (*right*) are masked out.

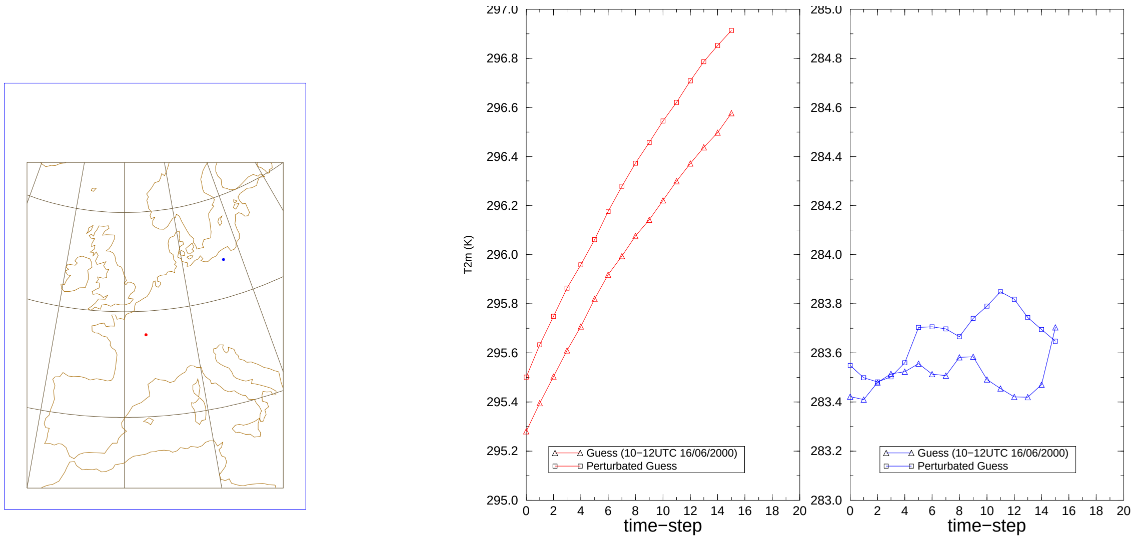

Figure 1: $2m$ temperature evolution in clear sky (Western point :47.27;3.10, left curves) and rainy situation (Eastern point: 53.70;17.01, right curves)

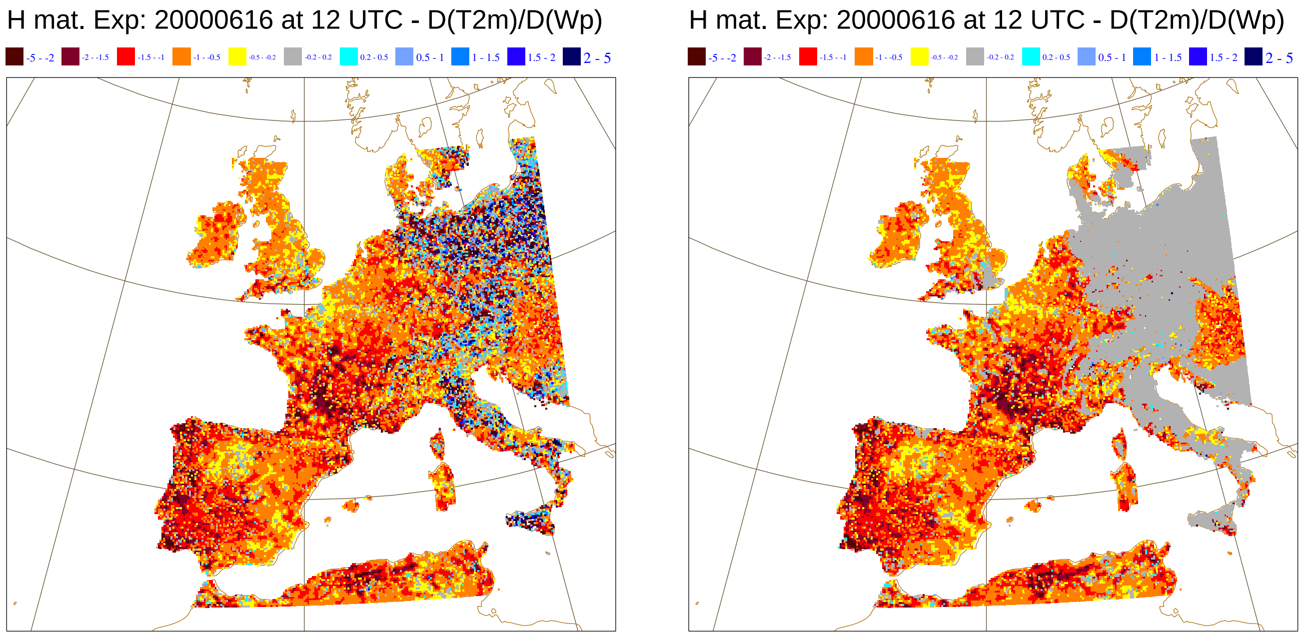

Figure 2: **H** matrix term at 12UTC of 20000616 - ΔT_{2m} / ΔW_p (K/m); left: no mask; right: mask of sensitive zones

Validation of the horizontal decoupling hypothesis

A validation test is designed to prove the horizontal decoupling hypothesis. The reference state of soil moisture W_{ref} is taken as the medium value *SWI*=0.5 over the entire domain of ALADIN-France and simulated observations are generated with a 6 hour forecast. The guess (with a modified soil moisture W_{mod}) is taken as *SWI*=0.75 within a box of about 400×400 *km* centred over France and *SWI*=0.5 elsewhere. Inside this main box four other boxes are placed (size 10×10 km at *SWI*=0.25, 20×20 km at *SWI*=0.25, 40×40 km at *SWI*=0.5 -equal to reference-, 60×60 km at *SWI*=0.25), to test different scales and to observe the influence on grid points close to the boxes. The model is initialised at 6 UTC and 6 hour forecast is produced. Results are plot in figure 3. The initial difference between the guess and the reference for the soil moisture is plot in figure (a). The difference between the guess and the reference in the $2m$ temperature and relative humidity at 12 UTC are plotted in figures (b) and (c). The analysis of soil moisture is then obtained at 12 UTC with the constraints elaborated.

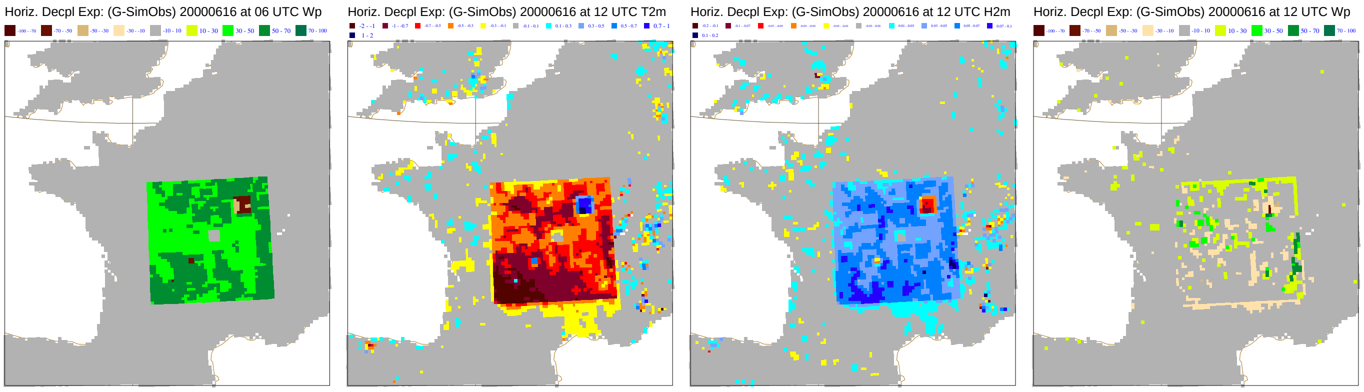

Figure 3: Test to assess the horizontal decoupling at 20000616 at 12 UTC for a modified initialisation of W_p at 6 UTC. The initial span W_{mod} - W_{ref} is shown in (a). (b) and (c) report the ΔT_{2m} and ΔHu_{2m} obtained after 6h integration (innovation vector for the soil moisture analysis). The residual error after the analysis done at 12 UTC ($W_{analysis}$ - W_{ref}) is given in (d)

The results show a net impact of the structure of W_p on the T_{2m} and Hu_{2m} fields with conservation of all scales features both for T_{2m} and Hu_{2m}. The boundaries present some extended signal of lower magnitude. The intensity of the signal depending on the horizontal scale of the box confirms also some small influence. Finally the analysis is able to retrieve the reference with good approximation in the inner box and reduced overshooting effect on the boundaries.

Conclusions and perspectives

It has been evaluated the use of a linearized variational technique for the total soil water content analysis from $2m$ simulated observation and for different time windows. The results are encouraging and further tests are necessary to validate the method with real observations. Particularly interesting is the 6h time window as it allows comparison with the statistical OI method. The study of the **H** matrix highlights several features related to synoptic situation. The mask of sensitive zones allows to further improve the convergence towards the reference state. In future work, the dynamically derived coefficients of correction provided by the variational method will be compared to the statistical OI coefficients used operationally.

2. Christopher SMITH : "Stability analysis and precision aspects of the boundary condition formulation in the non-hydrostatic dynamics and exploration of the alternatives for discrete formulation of the vertical acceleration equation both in Eulerian and Semi-Lagrangian timemarching schemes"

The latest results are described in the ALATNET report from Prague in this Newsletter.

3. Cornel SOCI : "Sensitivity studies using a limited-area model and its adjoint for the mesoscale range"

The investigations of the behaviour of the gradients at high resolution have been continued on the one hand to distinguish which was the mechanism for developing strong punctual sensitivities over the Alps in the so-called 'The Second French Storm' or 'T2' storm, and on the other hand the using of linearized simplified physical parameterization in adjoint ALADIN model. The accuracy of the linearization of the simplified physical parameterization has been compared with the nonlinear results.

Some comments regarding the 'T2' storm

When using a model integration area with high resolution, one of the characteristics is a better described orography. Also the parameterization of physical processes has to be able to simulate mesoscale feature of the atmospheric flow. During a strong advection, if high mountains barrier is encountered, strong gravity waves are generated. In this case, a numerical model will produce even higher energy coming from gravity waves than in reality. With a proper time step and a good physical description (e.g. surface drag and vertical diffusion) this energy is dissipated and the model remains stable.

For avoiding numerical instability in the computation of the gradients, the adjoint of a direct model needs also a proper physical description of the atmospherical processes. The difficulty of developing a complex adjoint model arise not from the linearization of the primitive equations but from the physical processes due to the strong nonlinearities and discontinuities. Buizza (1993) showed that an important physical parameterization for the adjoint models is the planetary boundary layer scheme. In our experiments, using adjoint of the ALADIN model, the results have shown that for a coarser domain (e.g. Irish Christmas Storm), the simple representation of the vertical diffusion and gravity wave drag was enough to prevent the development of non-physical structures in PBL. When using a high resolution area, this poor linear physics is no more sufficient.

The results for T2 storm have revealed very strong gradients without meteorological relevance. To get rid of this spurious structure, several sensitivity studies were followed, we recall the reducing of the Eulerian integration time-step from 40 to 10 s having no effect and, the changing of the trajectory truncation in the adjoint model. Also, a retuning of boundary layer height and the scale factor for the wind speed in the crudest linearized simplified physics has been performed. The results, has revealed that the later approach is more appropriate but the effect was not only on the non-meteorological structures but also on useful part of the gradients.

Trying to answer the question why they have appeared we have searched for a key in the 18-hours forecast. A temporal sequence of spatial vertical cross-section along a relative direction where the gradients with the biggest magnitude have occurred have shown at +6h the existence of a strong baroclinic region in the upwind part before the mountains. Immediately downwind there is a turbulent region as suggested the form of the isentrops. Using the adjoint model from +18 hours to +0, the gradients of the forecast error norm were computed. As the normal flow is westward, in adjoint the wind tend to advect perturbations eastward. The results has demonstrated that with the 60 s time-step, the model becomes unstable in the last few hours of backward integration, the magnitude of the gradients having an exponential increase. An explanation is that the strong wind existing in the last hours of the integration corroborated with the improper time-step have produced a model stability criterion violation. Since for 40 s the instability has vanished, although big but not unrealistic sensitivities have developed, it appeared the necessity of a better description of the physical processes in the adjoint model.

The more complex simplified physical parameterization scheme proposed by Janiskova et al. is based on the vertical diffusion equation with a first-order closure for the exchange coefficients. During their tests some spurious noise close to the surface have been noticed. It was discovered that this problem was derived from the vertical diffusion scheme, and especially from the function of Richardson number, f(Ri). To overcome the occurrence of the artificial noise, a modification of f(Ri) to ensure a smaller derivative by a factor 10 in the central part, around the point of singularity, Janiskova et al. tested and adopted for the tangent linear version of the vertical diffusion scheme.

Including the vertical diffusion and gravity wave drag schemes in the ALADIN adjoint model, the results after 3h of integration have shown a proper magnitude and pattern for the computed mesoscale gradients. Using a completely adiabatic adjoint model, the computed sensitivities have big values mainly under the model level 20, about 2800 m. This result also suggests the necessity of a better description of PBL processes in adjoint model. When the simple linearized physics is included with default values for the boundary layer height and the scaling factor for the wind stress, the gradients values diminish compared to the adiabatic case, but remain big enough not to be used like small perturbation in the initial conditions. Yet, the simplified physics produces the smoothest vertical profiles and they are the most efficient in damping the undesired spots of gradients over mountainous area. With retuned values, the simple linear physics produce vertical profiles close to those of the simplified physical parameterization case. Unfortunately, it was not possibly to carry out the 18h adjoint integration using simplified physical parameterization since it requires a huge computer memory for storing of the trajectory. Nevertheless the aim of this linearized physics is not so much for 18h sensitivity studies but for no more than 6h mesoscale gradients computation which should be useful for a future 4d-var assimilation in ALADIN model.

Towards a better precipitation forecast?

In fact, even if a posteriori, the improvement of the precipitation forecast could be seen as one of the latest but not the last challenge of using the mesoscale sensitivities. The questions to be answered include: (1) Could be improved a bad forecasted precipitation field without modifying the model initial humidity state variable ? (2) Using the gradients method for changing the initial conditions, it could be possible to re-forecast precipitation where the model was not able to produce but they did occur in reality? Maybe one of the questions should have the answer expected from simple consideration of model dynamics or physical parameterization. However, we are not going to search the answer in this part, but primarily in the analysis errors.

As a case study, two spring situations have been used. We consider they are relevant for our purpose. They were selected because the precipitation forecast was bad, both amount and localisation. The integration domain used in the following experiments was ALADIN-France operational, ($300\times300\times31$, $\Delta x=9.5$ km). The gradients of 6 hours forecast errors have been computed starting from the verification time, 06 UTC. By adjusting the initial model state with a fraction of the gradients, the final purpose was the improvement of the 6-hours precipitation forecast.

Validation and accuracy of the linearization of the simplified physical parameterization.

Using the Taylor formula the global mathematical correctness of the linearized code of the simplified physical parameterization for ALADIN model with respect to the nonlinear version was done. Starting from a defined initial state, x, the accuracy of the Taylor formula is computed in the vicinity of a trajectory which is a nonlinear forecast. The testing perturbation, dx, is chosen at random. The standard validation of the tangent linear code have been performed for 7 steps, with 60 s time-step. The gravity wave drag, vertical diffusion and stratiform precipitation schemes were successively switched on. The results have shown a good accuracy of the linearization when using the schemes individually or in combination.

Comparisons have been done for the 3-hours evolution, on one hand of perturbation computed with the tangent linear model, and on the other hand of the finite differences between two nonlinear predictions using the simplified physical parameterization package. If taken individually, the linearization is valid for each scheme. Also when combining vertical diffusion with gravity wave drag scheme.

The results show that the nonlinear model become unstable for the small perturbations. The degree of the instability of nonlinear model is case dependent. For a good linearity when using large scale precipitation scheme together with vertical diffusion and gravity wave drag, one has to activate the smoothing functions.

Gradients computation

The two synoptic cases considered in our study have a general feature namely the 6-hours time window for gradients computation. This was the limit enforced on one hand the technical reasons and on the other hand the requirement to work within a time window which is supposed to be used in a future variational assimilation.

For the experiments using the adjoint model, we were concerned with sensitivity pattern when including simplified physical parameterization for gradients computation. The results for several tests have revealed that a parameter having a strong influence in gradients computation is the minimum critical thickness for precipitating clouds (ECMNP inside the code). Moreover, as long as convective scheme is not included in the adjoint model, it contributes to the trajectory only. This makes the adjoint model including large scale precipitation scheme to be much more sensitive to the physics used for creating trajectory than an adjoint with the dissipative part of the physical parameterization.

Concluding remarks

Several experiments using simplified physical parameterization as well as tangent linear and adjoint versions have been carried out. Due to technical reasons, the time window chosen in our tests was mainly 6 hours.

A first set of experiments performed for the Second French storm, have revealed that the spurious gradients structure developed over the Alps when the simple physics is included in adjoint model, vanish if simplified physical parameterization scheme (vertical diffusion and gravity wave drag) is used. This result obtained for a 3-hours time window has demonstrated the necessity of including a more sophisticated physical parameterization in the adjoint model.

The validation of the linearization of the simplified physical parameterization, that is the dissipative part plus large scale precipitation, has been performed as well. The results have shown that the tangent linear model describing the evolution of a perturbation of the order of magnitude of analyse increments fit the finite differences between two nonlinear forecasts. The nonlinear model become unstable at small perturbation. To obtain a good accuracy it is necessary to use the smoothing function both in direct and tangent linear models.

An adjoint model including a more sophisticated description of the physical processes become very sensitive to the trajectory. This is the result obtained when in adjoint model, large scale precipitation scheme was included besides vertical diffusion and gravity wave drag. Also it has been revealed that even a posteriori it is very difficult to ameliorate a failure of a precipitation forecast without a direct changing of the specific humidity state variable. Future work will concentrate in the direction of improving the model humidity field using the adjoint method.

4. Klaus STADLBACHER : "Systematic qualitative evaluation of high-resolution non-hydrostatic model"

The second part of the first year in Ljubljana was mainly used for finding proper use of orography on high resolution to enable forecast fields, which can be used for evaluation. The crucial field is the vertical velocity field, which logically has big impact on the shape of the precipitation patterns.

Down to 5 km resolution no negative influence on the forecasted precipitation fields caused by orography can be found, neither in hydrostatic (H) nor in non-hydrostatic (NH) model runs. Further increasing of the resolution can cause unrealistic wavy precipitation patterns over the sea (see figure 1). This is true for both, H and NH runs as well.

The case which was chosen to try to investigate this problem is the 20.9.1999, which is part of one MAP-I(ntensive) O(bservation) P(eriod). The forecasting domain includes part of north-east Italy, western Slovenia and parts of north-west Croatia. Domain size is 79*79 points (without E-zone) and the main synoptic feature is a front which approaches from the west, had its main activity in northern Italy and was already weaker, when affecting the target domain. A semi-Lagrangian time-scheme was used and the length of the time-step was 30 seconds, while the horizontal resolution was approximately 2.5 km.

This front caused quite some precipitation in the western part of Slovenia, which was also forecasted by the model although the forecasted peaks are too high. Nevertheless the most important point remains the influence of the used orography on the smoothness of the forecasted precipitation fields, after it turned out that changes in the settings of the physics (like horizontal diffusion coefficients) or the geometry (larger domain) did not cure the problem. If the minimisation algorithm is used (e.g. Jerczynski's cost-function), while producing the "clim" files the negative impact can be reduced for the NH-run, but only if coupling is done from a non-hydrostatic run (see figure 2 - coupled from NH-5 km). In comparison to this, figure 3 shows the precipitation field if the NH model is coupled from H-5 km model (orography also with minimisation). For the hydrostatic run on 2.5 km however, the better (with minimisation) orography reduces the negative influence more significantly.

To get completely rid of this waves over the sea I also tried to use orography on coarser resolution than the other spectral fields. This means that the used orography, which is included in the "clim" files was produced on quadratic grid, while the other spectral fields were on linear grid, which in fact means an increase of the resolution by a factor of 1.5 . Thanks to Dominique and Ryad for giving support, how to correctly include this "new" orography. The results show that the use of the smoother orography (but still using the minimisation algorithm) gives the most realistic precipitation fields, which means, that additionally to the reduction of the "ocean" waves, also the mountainous northern part of the domain does not have that extreme differences of the amounts within short distance (see figure 4).

Another "problem" that appears when trying to evaluate the model (and especially the advantages of the non-hydrostatic version) is the fact that the differences between NH and H dynamics might be small when compared to differences that come from other sources, such as the resolution of the coupling model. Figures 5 and 6 should serve as an example to underline this fact. In figure 5 the difference field between NH and H fields for the 850 hPa temperature forecast is plotted, while in figure 6 the same is done for the difference between NH model coupled from 5 km and 11 km, respectively. It can easily be recognised, that NH and H forecasts are more similar than the NH forecasts from different coupling fields. The reason for the differences concerning the different coupling resolution might partly be caused by some kind of shift. So it won't be that easy to work out the advantages of the NH dynamics in an objective way, because besides the above mentioned problem additionally we have to deal with the fact that the density of observations is not high enough, if the resolution is already down to 2.5 km or lower (MAP database therefore has to play an important role).

The next steps will be to find the most proper coupling strategy (concerning the 'jumps' in resolution) and to investigate the model performance on several cases (in different synoptic situations), which were already chosen out of MAP.

See also : "*Non-hydrostatic vs hydrostatic on high resolution*", by Klaus Stadlbacher, in the proceedings of the 10th ALADIN workshop.

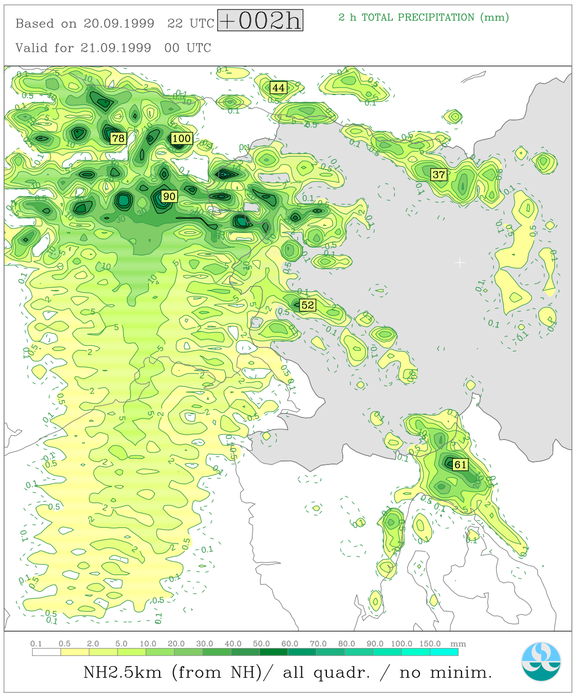

Figure1

NH with "normal" orography

coupled from NH-5km

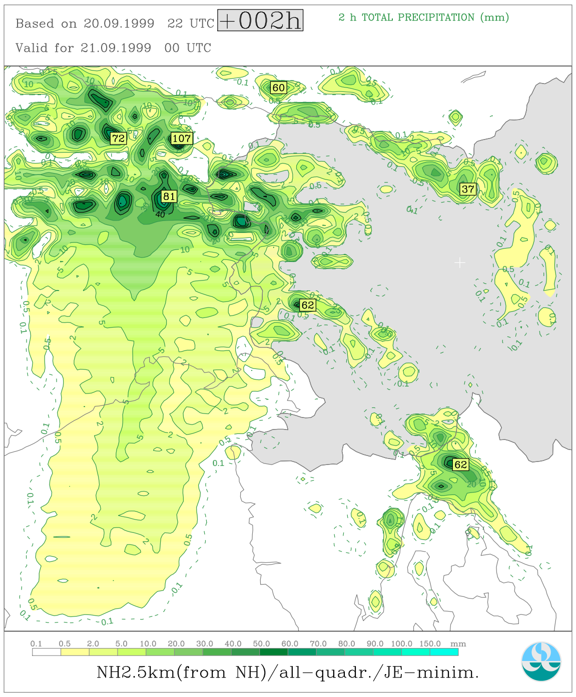

Figure 2

NH with "optimised" orography

coupled from NH-5km

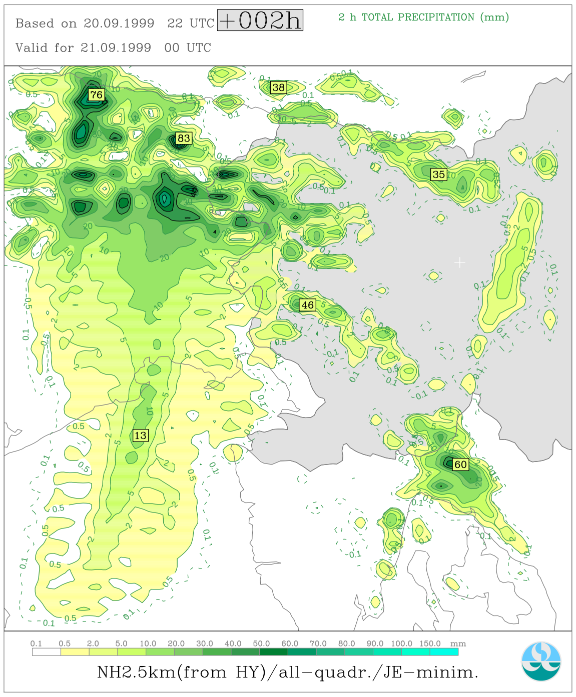

Figure3
NH with "optimised" orography
coupled from H-5km

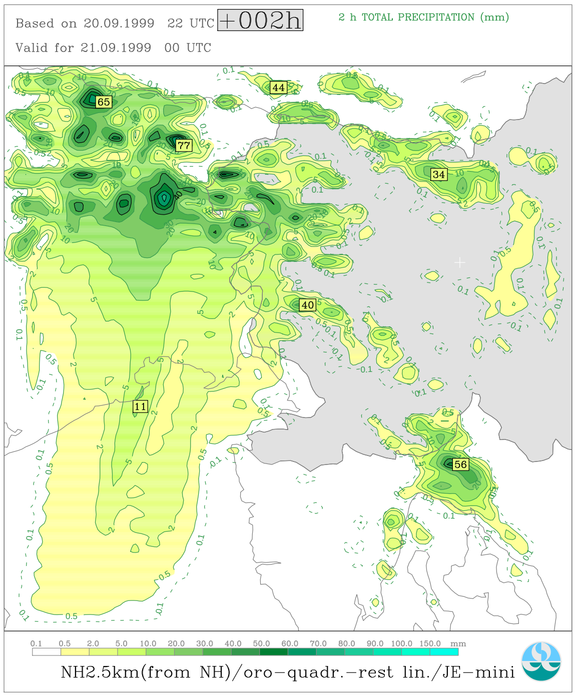

Figure 4
NH with smoother+"optimised" orography
coupled from NH-5km

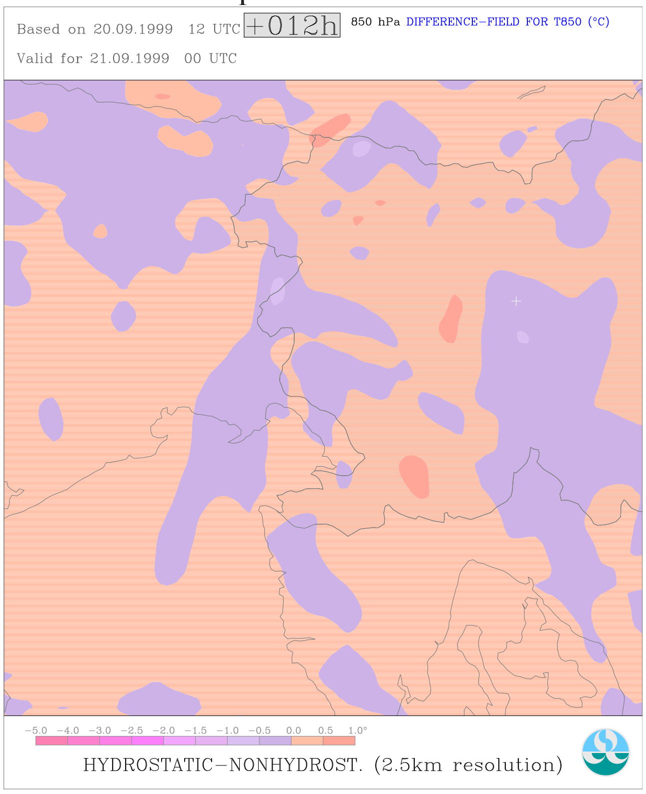

Figure 5
differ. between NH and H runs

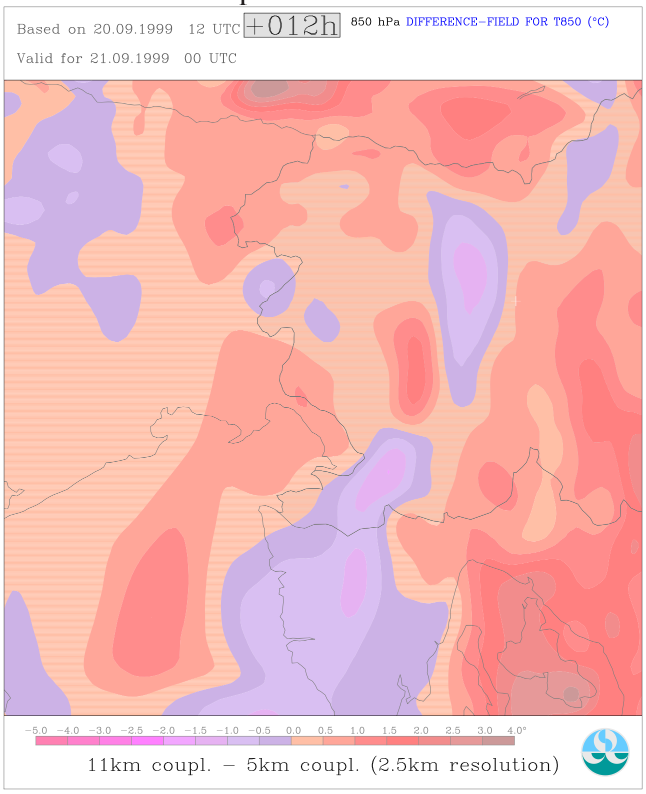

Figure 6
differ. between 11 km and 5 km coupling

5. Jozef VIVODA : "Application of the predictor-corrector method to non-hydrostatic dynamics"

The latest results are described in the ALATNET report from Prague in this Newsletter.

An improved method to incorporate lateral boundary conditions in a spectral limited area model

Gábor Radnóti, January 2001

Introduction

This study was stimulated by the famous "Christmas storms" of 1999 (26 and 27 December). In these cases two very intensive, rapidly propagating meso-scale cyclones, that developed over the middle Atlantic, passed Western Europe. The forecast of these systems failed in most global models, partly because around the times of cyclo-genesis only one observation over the Atlantic indicated the existence of the systems and most of the data assimilation schemes have rejected these observations. However, the French global model ARPEGE kept them and the cyclones were "reconstructed" by the assimilation procedure. Therefore the ARPEGE forecast of the "Christmas storms" was reasonably good, although the size of the systems was at the limit of scales that can be resolved by the global model ARPEGE.

In such a case one would naturally expect that a higher resolution limited area model (LAM) coupled with this basically correct global forecast performs even better in describing such a small scale system. However, it was not the case for ALADIN and the reason was easy to find. The quality of a forecast by a LAM is to a large extent determined by the quality of the coupling forecast. In the given case, a LAM has no chance to forecast the storm if the cyclo-genesis is outside its domain and at the same time the coupling model fails to forecast it. In such a case there is no way that the LAM gets any information through the lateral boundary conditions (LBC) on the existence and on the entry of the system to its domain. Even if the coupling model forecasts the system the coupling scheme may fail to pass the information to the LAM and it was the case for ALADIN for these storms. Most operational LAMs, including ALADIN, use the Davies relaxation scheme for the LBC treatment. In this scheme the global model forces the LAM only at a "narrow" bend at the lateral boundaries of the LAM domain. The width of this zone is typically at the range of 100 km. Additionally, the forcing field is not directly the forecasted field of the coupling model for the given time, but a field obtained by temporal interpolation between two forecasts of the global model (the time interval of interpolation is typically 3 or 6 hours). If the method is a simple polynomial (linear or quadratic) interpolation it may happen, and it was exactly the situation in the case of this study, that the system has no trace on the coupling zone within the time interval of the passage because at the initial time (T0) the system is fully outside the LAM domain and at the next coupling time (T1=T0+3h or T1=T0+6h) the system has already left the coupling zone and it is fully inside the domain. Since the coupling model passes information to the LAM only by its fields over the coupling zone at discrete times, the LAM has the chance to learn the entry of a system to its domain only if it had any trace on these spatially and temporally reduced sub-fields.

The aim of this study is to investigate the possibility to change the temporal interpolation scheme and/or the coupling scheme to overcome the limitations described above. The fact that ALADIN is a spectral model using Fourier expansions in both horizontal directions offers promising solutions. On the one hand we can change the temporal interpolation scheme by interpolating phase angles and amplitudes rather than gridpoint values. In this case at the interpolation step the complete fields of the coupling model are used and not only their projection on the coupling zone. Thus in principle it is possible to retrieve the approximate location and depth of a wave-like system at any time of the interpolation interval. The price that one has to pay for this is that of performing inverse Fourier transforms on the coupling fields at each time-step after the spectral interpolation. Such a solution may partly or fully solve the problem described. However, it may be the case that even such an improved interpolation is not capable for retrieving the trace of a system on the coupling zone, or that the Davies scheme does not perfectly passes to the LAM the characteristics of a small scale system entering the domain. If it is the case, there is a possibility to modify the Davies scheme by introducing an additional spectral coupling step. A spectral coupling scheme can be built up on the exact analogy of Davies scheme. The difference is that the relaxation scheme is introduced in the spectral space: small wavenumbers take over the role of coupling zone while large wavenumbers represent the inner zone of the Davies scheme. This procedure provides a scale selection where "large scales" are dominated by the spectra of the coupling model and the LAM dominates only the small scales poorly, or not at all resolved by the forcing model. In such a scheme scales resolved by the coupling model are forced to the LAM no matter what the location of a system of the given scale is within the domain. Therefore the LAM surely captures any system resolved by the coupling model and not only at the time of passage through a narrow lateral zone. This is a tempting potential advantage of spectral coupling. However, one can easily see that spectral coupling itself can not take over the role of LBC treatment, since even the expression "lateral boundary" is meaningless in the case of spectral coupling, where there is no geographical selection. Consequently spectral coupling can not eliminate spurious wave reflection from lateral boundaries (or in the case of a spectral LAM spurious inward wave propagation through the lateral boundaries), that is one of the primary aims of using coupling schemes. Nevertheless, one may hope that a careful simultaneous use of Davies scheme and a "well-tuned " spectral coupling can optimally combine the advantages of the two methods.

The following sections will discuss these possibilities with some spectral diagnostics and model tests on one of the "Christmas storm" cases.

Amplitude-phase-angle representation of ALADIN spectral fields to improve shape preserving properties of time-interpolation

The spectral representation of ALADIN fields is that coming from the subsequent one-dimensional FFTs (Fast Fourier Transform). As an example, when performing direct transformations, direct FFT is performed on each "latitude" and the resulting Fourier coefficients are transformed again by direct FFT along a "longitude". For a given zonal wavenumber the second transformation involves 2 FFTs, one performed for the real part and the other for the imaginary part. Therefore in the final result of the double FFTs a total wavenumber *(j,k) j,k=0* can be described by 4 independent coefficients:

$$\boldsymbol{Q}^{k}_{j_{rr}},\ \boldsymbol{Q}^{k}_{j_{ri}},\ \boldsymbol{Q}^{k}_{j_{ir}},\ \boldsymbol{Q}^{k}_{j_{ii}},$$

where *rr* means the real part of the second FFT on the real part of the first FFT, while *ri ir* and *ii* are the other three possible combinations. This representation is obviously not exactly the same as the coefficients in the two dimensional Fourier series:

$$Q(x,y)=\sum_{k=-\infty}^{\infty}\sum_{j=-\infty}^{\infty}Q^{j,k}\ e^{ijx}e^{iky}$$

(x, y being scaled into $[0, 2\pi]$). However, it is easy to deduce the conversion relationships between the two representations. The result is:

$$\begin{aligned}
Q_r^{j,k} &= \boldsymbol{Q}_{j_{rr}}^{k} - \boldsymbol{Q}_{j_{ii}}^{k} & Q_i^{j,k} &= \boldsymbol{Q}_{j_{ri}}^{k} + \boldsymbol{Q}_{j_{ir}}^{k} \\
Q_r^{-j,k} &= \boldsymbol{Q}_{j_{rr}}^{k} + \boldsymbol{Q}_{j_{ii}}^{k} & Q_i^{-j,k} &= \boldsymbol{Q}_{j_{ri}}^{k} - \boldsymbol{Q}_{j_{ir}}^{k} \\
Q_r^{j,-k} &= \boldsymbol{Q}_{j_{rr}}^{k} + \boldsymbol{Q}_{j_{ii}}^{k} & Q_i^{j,-k} &= -\boldsymbol{Q}_{j_{ri}}^{k} + \boldsymbol{Q}_{j_{ir}}^{k} \\
Q_r^{-j,-k} &= \boldsymbol{Q}_{j_{rr}}^{k} - \boldsymbol{Q}_{j_{ii}}^{k} & Q_i^{-j,-k} &= -\boldsymbol{Q}_{j_{ri}}^{k} - \boldsymbol{Q}_{j_{ir}}^{k}
\end{aligned} \tag{1}$$

$$\begin{aligned}
\boldsymbol{Q}_{j_{rr}}^{k} &= (Q_r^{j,k} + Q_r^{-j,k})/2 \\
\boldsymbol{Q}_{j_{ri}}^{k} &= (Q_i^{-j,k} + Q_i^{j,k})/2 \\
\boldsymbol{Q}_{j_{ir}}^{k} &= (Q_i^{j,k} - Q_i^{-j,k})/2 \\
\boldsymbol{Q}_{j_{ii}}^{k} &= (Q_r^{-j,k} - Q_r^{j,k})/2
\end{aligned} \tag{2}$$

When linear interpolation is performed between two fields the result is the same no matter if it is performed on the gridpoint values or on the spectral coefficients, and no matter which one of the above described two spectral representations is used (this is because both FFT and (1) (2) are linear in $\boldsymbol{Q}$). Another possibility would be to perform the interpolation between amplitudes and phase-angles. The potential advantages and problems related to this will be discussed later. Now we want to see how one can obtain such a representation from the standard one. First let us consider the 1 dimensional case:

The amplitude phase angle representation means that a wave is described by $A_j \sin(jx + \lambda_j)$. This means that for a wavenumber $j > 0$:

$$\boldsymbol{Q}^{j} e^{ijx} + \boldsymbol{Q}^{-j} e^{-ijx} = A_j \sin(jx + \lambda_j) \tag{3}$$

must hold, the left hand side being the cumulated contribution of wavenumber j in the 1 dimensional Fourier series :

$$\sum_{j=-\infty}^{\infty} Q^j e^{ijx} .$$

Consequently :

$$Q^j e^{ijx} + Q^{-j} e^{-ijx} = Q^j{}_r e^{ijx} + iQ^j{}_i e^{ijx} + Q^{-j}{}_r e^{ijx} + iQ^{-j}{}_i e^{-ijx} = A_j \sin(jx + \lambda_j)$$

$$\Downarrow$$

$$\begin{aligned}
&Q_r^j \cos(jx) + iQ_r^j \sin(jx) + iQ_i^j \cos(jx) - Q_i^j \sin(jx) + \\
&Q_r^{-j} \cos(jx) - iQ_r^{-j} \sin(jx) + iQ_i^{-j} \cos(jx) + Q_i^{-j} \sin(jx) = A_j \sin(jx + \lambda_j)
\end{aligned}$$

The left hand side contains imaginary terms that must vanish. This leads to the complex conjugate relationship between positive and negative indices. Then we obtain :

$$A_j^{\,2} = 4\boldsymbol{Q}_r^{j\,2} + 4\boldsymbol{Q}_i^{j\,2}, \qquad \lambda_j = \begin{cases} \mathrm{arctg}\left(-\dfrac{\boldsymbol{Q}_r^j}{\boldsymbol{Q}_i^j}\right) & \text{if } \boldsymbol{Q}_r^j > 0 \\ \pi + \mathrm{arctg}\left(-\dfrac{\boldsymbol{Q}_r^j}{\boldsymbol{Q}_i^j}\right) & \text{otherwise} \end{cases} \tag{4}$$

Now let us consider the problem in two dimensions. Analogously to (3) the Fourier series contributes to a positive wavenumber pair j, k >0:

$$Q^{j,k} e^{i(jx+ky)} + Q^{-j,-k} e^{-i(jx+ky)} + Q^{j,-k} e^{i(jx-ky)} + Q^{-j,k} e^{-i(jx-ky)} \tag{5}$$

On the analogy of (3) the first two terms of (5) define a wave with amplitude and phase angle $A_{j,k}$, $\lambda_{j,k}$ and the second two terms another wave with amplitude and phase angle $B_{j,k}$, $\mu_{j,k}$, and the result is a superimposition of the two plane waves:

$$\begin{aligned} Q^{j,k} e^{i(jx+ky)} + Q^{-j,-k} e^{-i(jx+ky)} &= A_{j,k} \sin(jx+ky+\lambda_{j,k}) \\ Q^{j,-k} e^{i(jx-ky)} + Q^{-j,k} e^{-i(jx-ky)} &= B_{j,k} \sin(jx-ky+\mu_{j,k}) \end{aligned} \qquad (6)$$

Then the counterpart of (4) is :

$$A_{j,k}^2 = 4Q_r^{j,k\,2} + 4Q_i^{j,k\,2}, \qquad \lambda_{j,k} = \begin{cases} \operatorname{arctg}\left(-\dfrac{Q_r^{j,k}}{Q_i^{j,k}}\right) & \text{if } Q_r^{j,k} > 0 \\ \pi + \operatorname{arctg}\left(-\dfrac{Q_r^{j,k}}{Q_i^{j,k}}\right) & \text{otherwise} \end{cases}$$

and (7)

$$B_{j,k}^2 = 4Q_r^{j,-k\,2} + 4Q_i^{j,-k\,2}, \qquad \mu_{j,k} = \begin{cases} \operatorname{arctg}\left(-\dfrac{Q_r^{j,-k}}{Q_i^{j,-k}}\right) & \text{if } Q_r^{j,k} > 0 \\ \pi + \operatorname{arctg}\left(-\dfrac{Q_r^{j,-k}}{Q_i^{j,-k}}\right) & \text{otherwise} \end{cases}$$

and reversely :

$$\begin{aligned} Q_r^{j,k} &= A_{j,k} \sin(\lambda_{j,k})/2 \\ Q_i^{j,k} &= -A_{j,k} \cos(\lambda_{j,k})/2 \end{aligned}$$

(8)

$$\begin{aligned} Q_r^{j,-k} &= B_{j,k} \sin(\mu_{j,k})/2 \\ Q_i^{j,-k} &= -B_{j,k} \cos(\mu_{j,k})/2 \end{aligned}$$

For the set of *(j,k)* plane waves the total wavenumber direction is in the first quarter of the plane, while the set of *(j,-k)* pairs falls in the fourth quarter. It means that the total set of the waves spans the half-circle, as it can be expected:

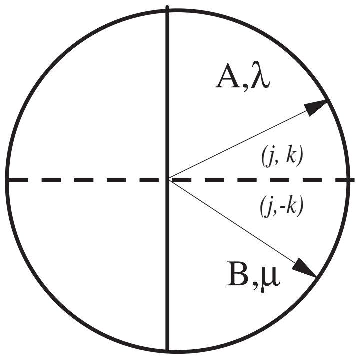

If j=0 or k=0 (but not both are zero), then (5) contains only 2 terms and the problem reduces to the one dimensional case. Then the first two equations of (7) and (8) are sufficient. The missing pairs *(-j,k)* and *(-j,-k)* of (8) can be determined from the complex conjugate relationships. The combination of (1) and (7) provide the conversion formula in one direction and the combination of (2) and (8) in the opposite direction. Then the temporal interpolation between the spectral fields can be realized by a 3 step algorithm: for each wavenumber pair the two phase-angle amplitude pairs are computed, then the interpolation is performed between amplitudes and angles, finally the so obtained new amplitudes and phase angles are transformed back to obtain the new spectral coefficients.

The potential advantage of such a scheme can be illustrated on Fig. 1 in one dimension:

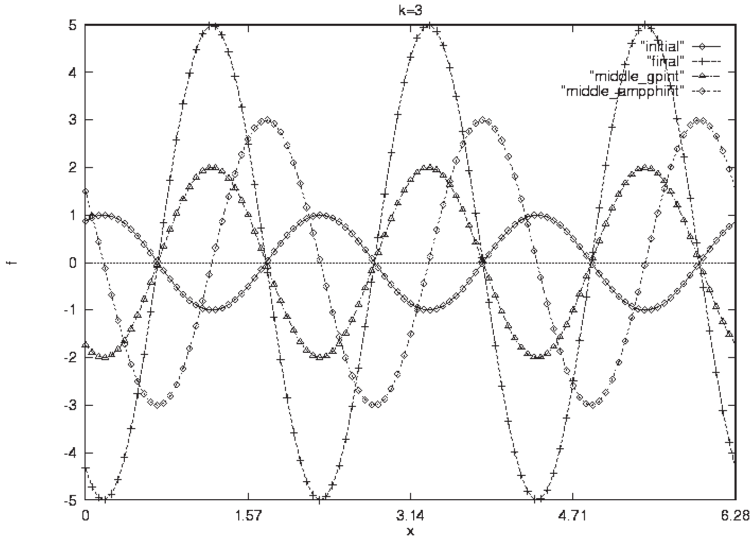

Figure 1 : A single wave (wavenumber=3) at initial, final time and at middle time obtained with different interpolations

We can see four waves with wavenumber 3. We defined a wave with a given amplitude and phase as an initial wave and another one with an increased amplitude and shifted phase as a final wave. Let us assume that we want to estimate the state of the evolving wave in the middle of the time interval. It is reasonable to assume that it is the amplitude and the phase of the wave that evolve linearly rather than the gridpoint values. The first assumption leads to the interpolated wave denoted by squares and the second leads to the curve denoted by triangles (and exactly this second curve would be obtained if spectral coefficients were interpolated). We can see that the two results differ significantly: The second choice results in a wave that is in phase very close to the final wave, while the first choice by definition results in a wave which is exactly in middle phase with middle amplitude. The reason for the "failure" of gridpoint interpolation is that the final wave is significantly stronger than the initial one. Consequently, the result of interpolation, as far as phase angle is concerned, is dominated by the final state. In reality one may think that the wave is deepening gradually and this is the most advantageous feature of phase angle/amplitude interpolation.

It is a little bit more interesting to see the same problem for a wave packet. Fig. 2 illustrates an initial wave packet and its future state.

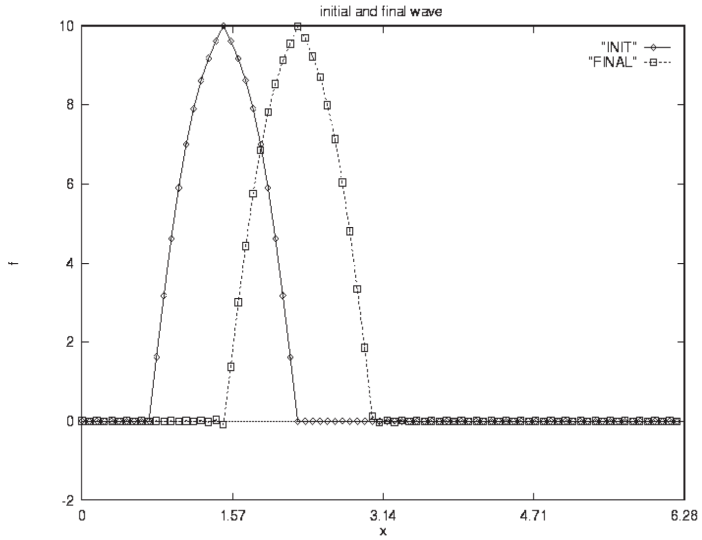

Figure 2 : A wave packet at initial and final time: phase speed is constant

For the sake of simplicity here we assumed a constant phase speed, which in this case is equal to the group velocity, and we also assumed time independent amplitudes for each wave component. Therefore the whole simple structure propagates in time without any deformation. Then we performed time interpolation to the middle time. Fig. 3 shows the result of linear interpolation for the middle time together with the initial state.

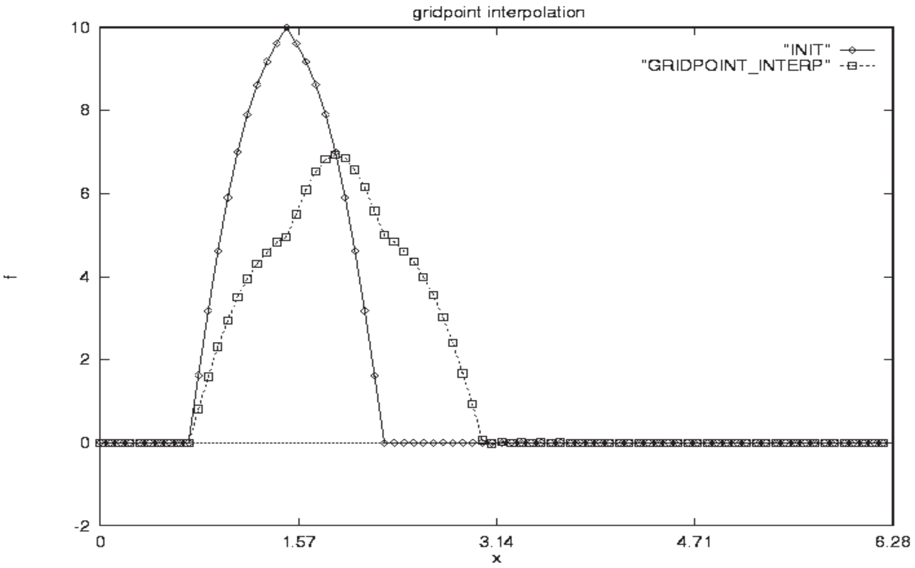

Figure 3 : Result of gridpoint interpolation and the initial wave packet

We see that the interpolation strongly modifies the shape of the wave packet. When we want to improve it by interpolating phase angles a serious aliasing problem occurs: Although the whole system propagated only by $\pi/4$, for a single wave of wavenumber k the shift in phase angle is $kx\pi/4$, that is already for relatively small wavenumbers bigger than $2x\pi$. If the interpolation does not take into account this fact (phase angle of final state is converted into $[0\,, 2x\pi]$ and interpolation is in the shorter direction between the two phases) the result of phase angle interpolation is seen on Fig. 4, which is the worst among all.

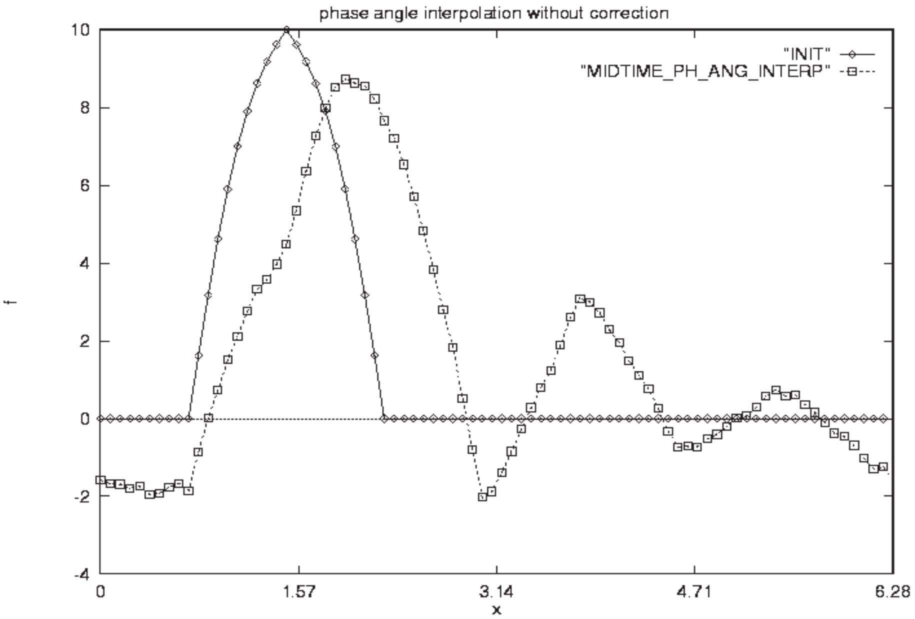

Figure 4 : Result of phase angle interpolation (modulo is neglected) and initial wave packet

However, if the modulo (number of 2π**ERREUR : Type de champ inconnu** passages) is taken into account the result, as expected, is perfect (Fig. 5).

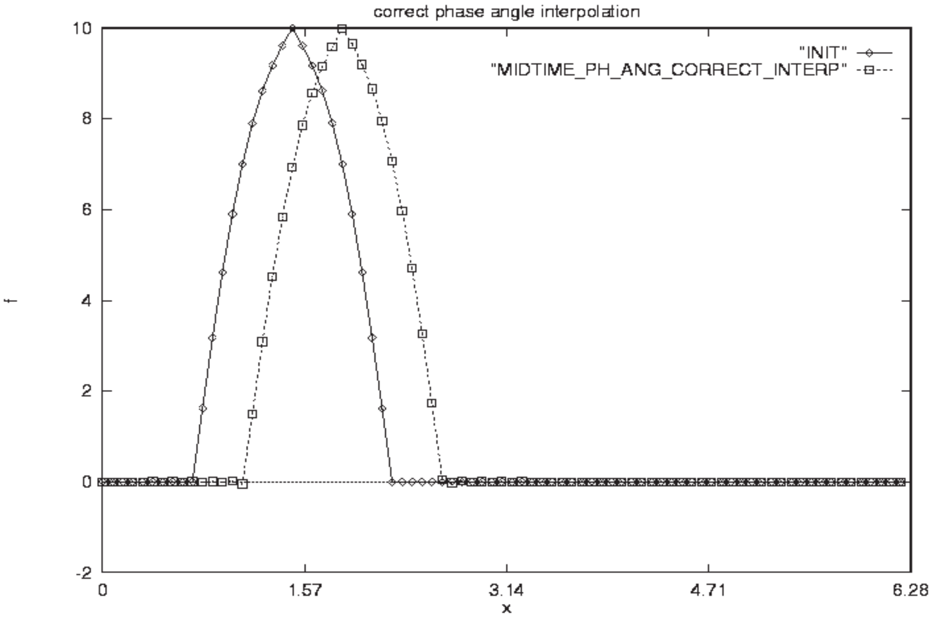

Figure 5 : Result of phase angle interpolation (modulo taken into account) and initial wave packet

To take the modulo exactly into account is not easy in the general case when the phase speed and the group velocity varies with the wavenumber and also with time, i.e. the temporal evolution is dispersive. It is a problem that has to be deeply analysed. In the NWP framework a first-order approach can be that for each wavenumber (in 2 dimensions for each wavenumber pair) the one time-step tendency of the corresponding phase angles provides an estimation for the total phase shift of the given time-interval. From this one can estimate the number of full periods of phase angle in that time interval to be added to the phase angle of the final state before doing the time interpolation. This can work well only if the phase speed of a given wavenumber pair does not strongly vary within the time interval. This can be true in most cases, but perhaps not in the most extreme situations, which are in the scope of our main interest in this study.

Let us assume that an intensive, relatively small scale system is rapidly approaching the domain of integration. It is reasonable to believe that the propagation speed of the system is strongly linked to the group velocities around the typical scale of the system. However at the initial time, when the phase speeds are estimated from the model tendencies, the given system has not yet reached the model domain therefore the extrapolation of these phase speeds to a time when the system is fully inside the domain might be misleading. With other words, the phase speeds may have a sharp change around the time when the system enters the domain. Another problem is that this method would assume that the phase speeds of the coupling model are the same as those of the coupled one, since the estimation is from the coupled model tendencies and it would be applied for the coupling fields.

The above described problems may be a major drawback of the proposed method. However, it is something to be carefully studied by a spectral analysis of model fields.

Another method can be also tested to estimate the modulo: although the phase speeds and group velocities vary with wavenumber, one can assume that it has some regularity that permits the persistence of wave packets. This may help to find the correct modulo: we may also assume that at the smallest wavenumbers the modulo is 0 or ±1 (the longest waves do not travel more than a full wavelength within a few hours). In one dimension we have the relationship :

$$-c(k) = (\lambda(k,\mathrm{T}) + 2\,n(k)\,\pi - \lambda(k,0)) / k\mathrm{T} \qquad (9)$$

where c is the phase speed, λ is the phase angle, k is the wavenumber, n is the modulo within the time interval T of interpolation. We assume that for "small" wavenumbers $n(k) = 0$, 1 or -1, that one is chosen which results in the minimal $| c(k) |$ (this means that the "shorter" phase direction is chosen between the initial and final phase angle). This estimation for small wavenumbers is reliable because here the denominator in (9) is relatively small, so changing the numerator by 2π would surely result in an unrealistically large phase speed. So we may assume that for $k = 1, 2$ we have a good estimation of $c(1)$ and $c(2)$. We continue on, apply (9) for the step by step increased wavenumbers keeping $n(k)$ on its initial $n(1)$ value as long as there is a sharp change in $c(k)$ or rather in the group velocity $c_g(k) = (k+1)\, c(k+1) - k\, c(k)$. Then we eliminate this jump by increasing or decreasing $n(k)$ by one. Algorithmically it means that from $c(k)$ and $c_g(k-1)$ we give an extrapolation for $c(k+1)$, then we compute $c(k+1)$ by using $n(k+1)=n(k)$, $n(k+1)=n(k)+1$ and $n(k+1)=n(k)-1$ from (9) and that one of the three results is accepted which is closest to the extrapolated value. This is the one dimensional algorithm and it has to be generalized for 2 dimensions. The generalization may be done by the use of (6). Similar procedure can be introduced as described above. However, it is reasonable to simplify the problem in two dimensions and to use only the fundamental phase speed for computing the modulo for both waves represented in (6) : for the first wave in (6) one has :

$$A_{j,k}(t) \quad \sin\left(jx + ky + \lambda_{j,k}(t)\right) = A_{j,k}(t) \sin\left(jx + ky + \lambda_{j,k}(0) - \omega_{j,k} t\right) \qquad (10)$$

where $\omega_{j,k}$ is the angular velocity of the wavenumber pair (j,k).

From this we obtain :

$$\omega_{j,k} = (\lambda_{j,k}(\mathrm{T}) + 2 n_{j,k} \pi - \lambda_{j,k}(0)) / \mathrm{T} \qquad (11)$$

The fundamental phase speed can be defined as :

$$c_{j,k} = \frac{\omega_{j,k}}{\sqrt{(j2\pi/\mathrm{L}_x)^2 + (k2\pi/\mathrm{L}_y)^2}} \qquad (12)$$

where L_x and L_y are the domain sizes in x and y directions respectively. The algorithm for computing the modulo is then analogous to the one dimensional case :

- For wavenumber pairs (1,1), (1,2) and (2,1) we use $n_{j,k} = 0, \pm 1$, and for each we select the one giving the minimal total phase-speeds
- We gradually increase j and k and extrapolate according to a first order Taylor expansion: $c_{j,k} = c_{j-1,k} + c_{j,k-1} - c_{j-1,k-1}$
- We compute (12) using $n_{j,k} = n_{j-1,k} = 0, \pm 1$, $n_{j,k} = n_{j,k-1} = 0, \pm 1$, and select that value of $n_{j,k}$ which gives the closest result to the extrapolation

Preliminary tests of the method by spectral diagnostics

The first thing to test is the mathematical correctness of the phase-angle/amplitude representation introduced in the previous section. To do this we took one of the spectral fields (temperature of the lowest model level), applied equation (1) and (7) and computed temperatures for each gridpoint by :

$$T(m,n) = \sum_{j=0}^{JMAX} \sum_{k=0}^{KMAX(j)} \left[A_{j,k} \cdot \sin(j2\pi\frac{m-1}{M} + k2\pi\frac{n-1}{N} + \lambda_{j,k}) + B_{j,k} \cdot \sin(j2\pi\frac{m-1}{M} - k2\pi\frac{n-1}{N} + \mu_{j,k}) \right] \qquad (13)$$

where m,n are the gridpoint indices, M,N are the total number of gridpoints in x and y directions and *JMAX* and *KMAX(j)* are the maximum wavenumbers that are specified by the type of truncation, that is elliptic truncation in our case (the rest of notations is as before). We compared the so obtained temperatures with the ones obtained by the standard inverse Fourier transforms and the results were identical (maximum difference of the two gridpoint fields over the whole domain was of the order of 10^{-13}).

Before applying the method for the ALADIN system we wanted to see the impact of the improved interpolation method on an idealized case in a spectral shallow water model. This model uses exactly the same spectral representation of wind speed and geopotential as the ALADIN model. The model runs on fully periodic fields without coupling.

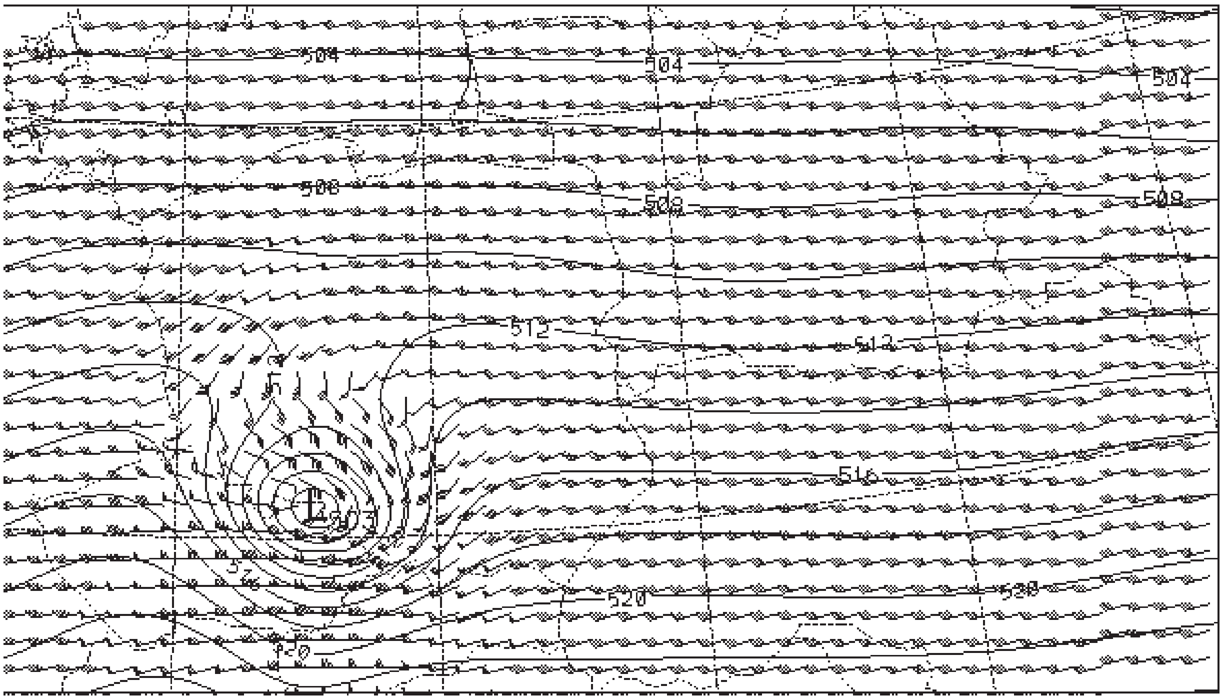

Figure 6.a : Zoom of a 12 hour integration of the spectral shallow water model

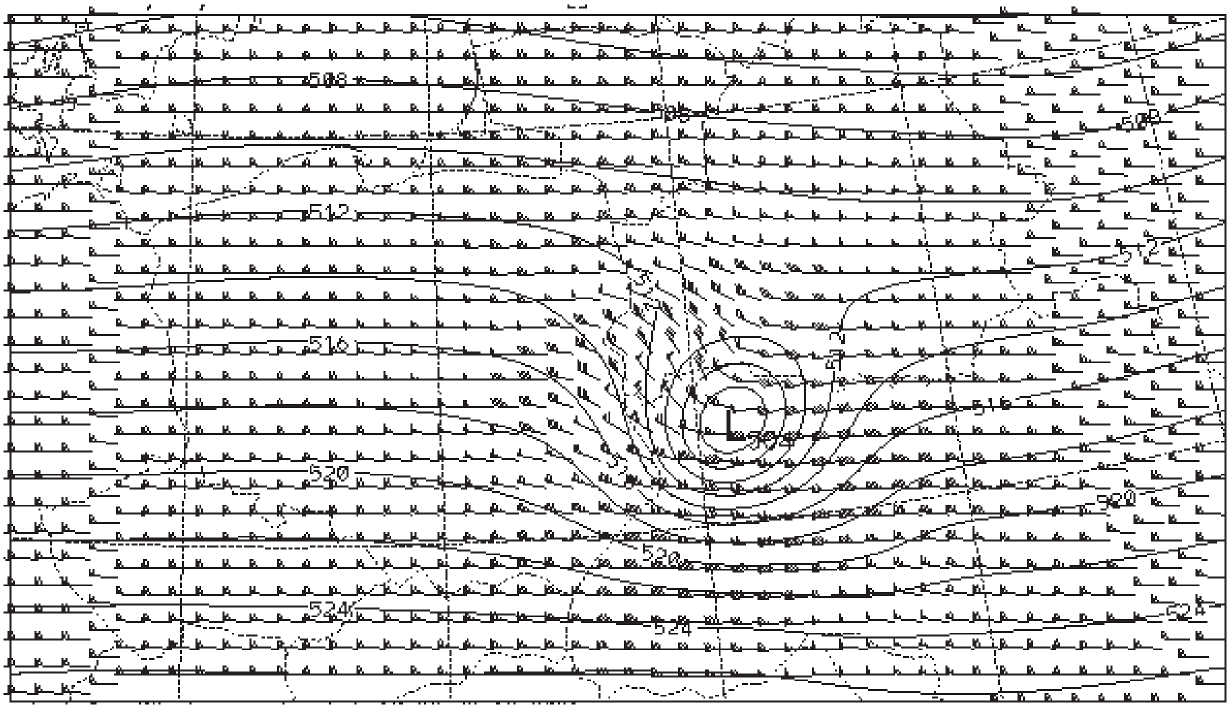

Figure 6.b : Zoom of a 18 hour integration of the spectral shallow water model

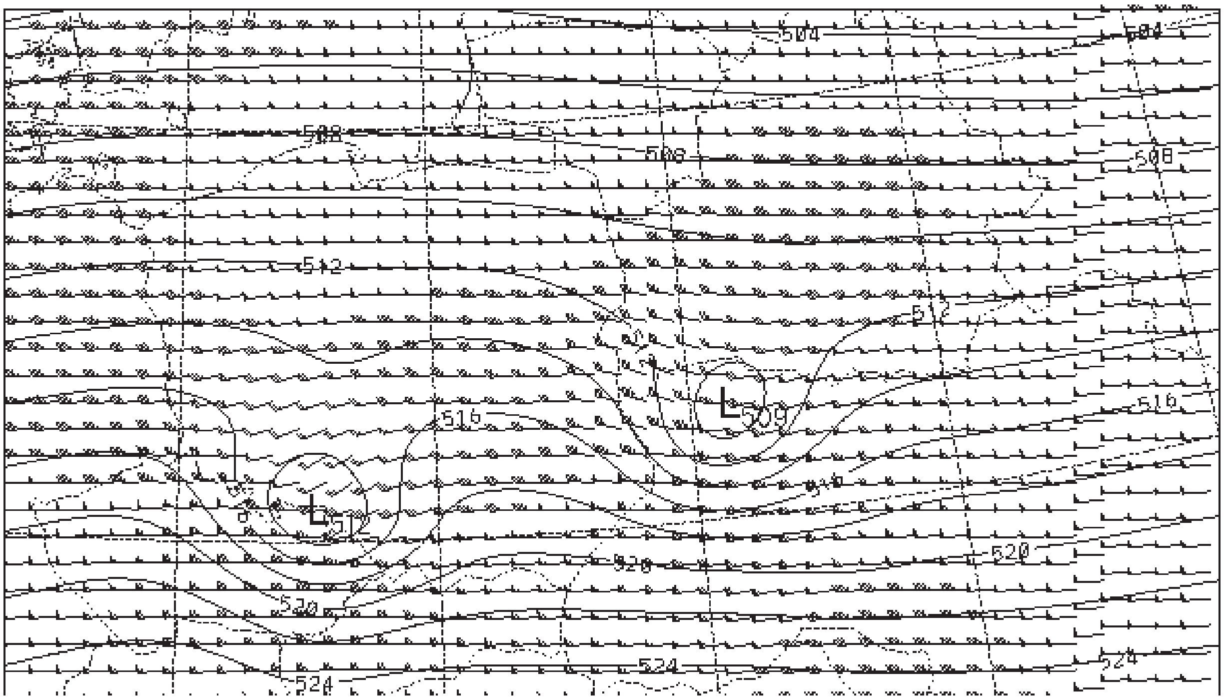

Figure 6.c : Zoom of gridpoint interpolation between 12h and 18h forecasts

As an initial state we have chosen a constant meridional geopotential gradient on the northern half domain and its opposite in the southern part to fulfil periodicity requirement. Then we put a perfectly circular cyclone over the northern part of the domain and we started from geostrophic balance. Then we used nonlinear normal mode initialization and integrated the model for 24 hours. To compare the two interpolation methods we have chosen the 12 and 18 hour forecasts. A zoom of the "active" area can be seen on Figure 6.a (12 hour forecast) and Figure 6.b (18 hour forecast). We can see that the cyclone is rapidly travelling eastward; in 6 hours it moved more than its characteristic size. Figure 6.c shows the result of linear gridpoint interpolation to middle of the time interval.

As we can see the interpolation is unsatisfactory: Instead of the propagation of the system we see that the initial cyclone is dying out and simultaneously the final cyclone is building up. If we assume that there is LAM embedded into this domain with a lateral boundary zone laying between the initial and final location of the cyclone, obviously this interpolation method will not pass any information on the entering cyclone.

Now let us see how the amplitude/phase angle interpolation performs for the very same case. At first we have visually analysed initial and final phase angle sets to get a first impression if the assumptions introduced in the previous section hold. We printed out initial and final phase angles of wavenumber pairs *(j,j)* (plane waves with NW-SE constant phase lines). The following table shows the results:

(j,k) : (1, 1)	λ(12h) of Φ : 286	λ(18h) of Φ : 150	estimated number of 2π passages : 0
(2, 2)	213	9	0
(3, 3)	141	267	-1
(4, 4)	97	210	-1
(5, 5)	132	81	-1
(6, 6)	78	305	-2
(7, 7)	39	196	-2
(8, 8)	357	95	-1
(9, 9)	320	342	-2
(10,10)	284	234	-2
(11,11)	256	119	-2
(12,12)	221	3	-2
(13,13)	189	248	-3
(14,14)	160	133	-3
(15,15)	129	15	-3

From the table we can see that phase speeds evolve quasi-regularly up to wavenumber pair (15,15) and it suggests that the algorithm proposed in the previous section might work well. It means that 2π passages can be safely identified for relatively small wavenumbers. At the second part of the spectrum it is not absolutely true, but we may hope that phase errors at those very small scales do not spoil the overall results because on the one hand the corresponding amplitudes are small and on the other hand phase error at a wave with very short wave length results only in a "few kilometre" shift of the given wave. After this "ad hoc" preliminary diagnosis the amplitude / phase angle interpolation was performed by the use of a slightly simplified version of the above proposed algorithm. The result can be seen on Figure 6.d .

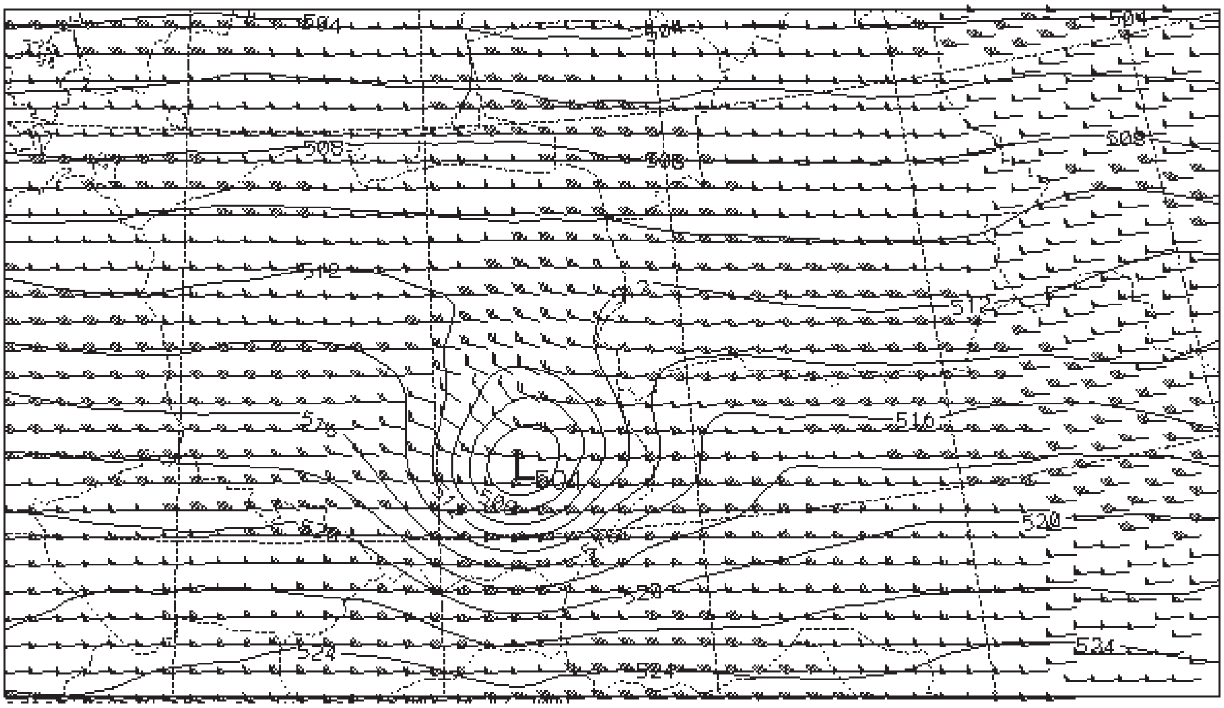

Figure 6.d : Zoom of amplitude / phase angle interpolation between 12h and 18h forecasts

We can see that the interpolation is much better than the gridpoint interpolation: the cyclone track is well represented without any artificial weakening, that was an undesirable feature of the gridpoint interpolation results.

After this we repeated the tests for ALADIN with one of the Christmas storm cases. In this case, unfortunately, the phase angles did not indicate any regularity for non of the state vector components. We also tested one time-step tendencies of phase angles computed inside the model, but these neither indicated any persistence. Therefore we could try amplitude/phase angle interpolation only without unaliasing algorithm. The results of amplitude/phase angle and gridpoint interpolation were surprisingly similar (Figure 7.a-c).

The first two figures show how the mesoscale cyclone was rapidly moving, but the interpolation significantly smoothed it out and we can see the "bipole" structure, although not so strongly as in the gridpoint interpolation on the shallow water model results. It has to be mentioned that the interpolation was not directly performed on mean sea level pressure, but on the model state vector components and mean sea level pressure was obtained only afterwards by post-processing. It is very probable that the pure state vector components are not suitable for such a method, since its components do not clearly exhibit "propagating wave" structure. One has to investigate how the state vector should be transformed before the interpolation to take the benefit indicated by the shallow water experiments.

Parallelly we plan to investigate the possibility of combining standard coupling scheme with spectral coupling and the overall impact of amplitude-phase angle interpolation combined with Davies coupling.

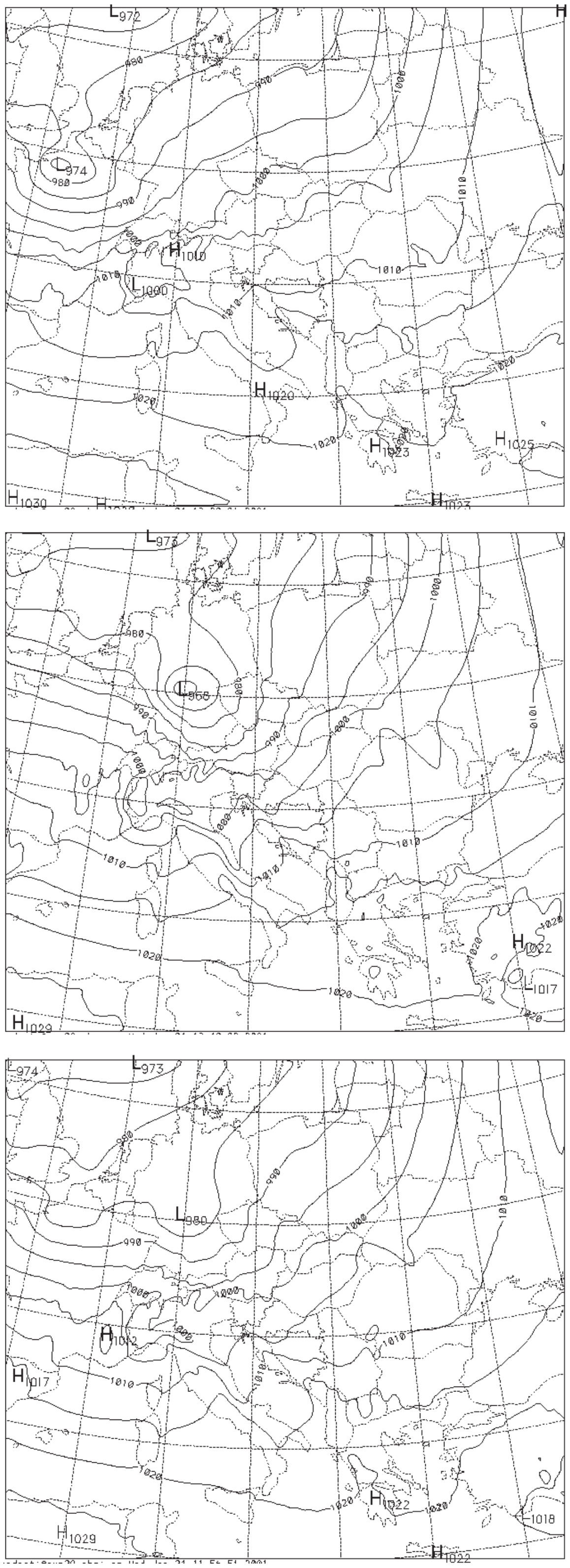
a b c

Figure 7 : a. 18 hour mean sea level pressure forecast ; b. 24 hour mean sea level pressure forecast ; c. Result of amplitude phase angle interpolation

Tendency coupling of the surface pressure

Tamás Szabó

1. Introduction

The interpolation from the large scale model's orography to the nested model's one can cause imbalance in the surface pressure. If this happens in the coupling zone, the unbalanced pressure will be coupled. To decrease this harmful effect we implemented a tendency coupling scheme for the surface pressure. For more details about this topic see Szabó (2001).

2. Coupling schemes in ALADIN

First it is worth comparing the old and the presently used coupling schemes.

2.1 The old t0 coupling scheme

This relaxation scheme was applied at the beginning of the gridpoint computations, so the derivatives also had to be modified, furthermore the gridpoint computations had to be done in the extension zone as well, otherwise biperiodicization would have been needed. The scheme was:

$$Q_c^0 = (1-\alpha)Q^0 + \alpha Q_{LS}^0 \qquad (1)$$

$$\left(\frac{\partial Q^0}{\partial x}\right)_c = \frac{\partial Q^0}{\partial x} + \alpha\left(\frac{\partial Q_{LS}^0}{\partial x} - \frac{\partial Q^0}{\partial x}\right) + \frac{\partial \alpha}{\partial x}\left(Q_{LS}^0 - Q^0\right) \qquad (2)$$

where α is the relaxation coefficient (Janisková 1994), Q is the model state vector, and the subscripts c and LS stand for coupled and large scale, respectively.

2.2 The presently used t1 coupling scheme

This scheme is applied after the gridpoint computations, just before the spectral transforms at the level of the SI equation, which is as follows:

$$(I - \beta\,\Delta t\,L)Q^+ = Q_E^+ + \delta Q_{ESI}^+ = Q_{RHS}^+ \qquad (3)$$

where Q_E^+ is the explicit guess, δQ_{ESI}^+ is the explicit part of the semi-implicit correction (see Bénard 1999), Q_{RHS}^+ contains the whole RHS of the equation and L is the linear model. The gridpoint computations are not needed to be done in the extension zone, since the coupling scheme makes the fields biperiodic. The scheme is applied on intermediate quantities, not on the prognostic variables themselves (Radnóti 1995):

$$\left[(I - \beta\Delta tL)Q^+\right]_c = (1-\alpha)Q_{RHS}^+ + \alpha(I - \beta\Delta tL)Q_{LS}^+ \qquad (4)$$

The coupled variables have to be similar quantities, thus the presence of the *(I - β∆t L)* operator on the LHS of the SI equation shows that this operator has to be applied on Q^{+}_{LS} before coupling in (4).

2.3 Comparison of the two schemes

The two above-mentioned coupling schemes are not equivalent:

$$Q_c^+ = F^{-1}D(I-\beta\Delta tL)^{-1}TF\left[(1-\alpha)Q^+_{RHS} + \alpha(I-\beta\Delta tL)Q^+_{LS}\right] \neq$$
$$(1-\alpha)F^{-1}D(I-\beta\Delta tL)^{-1}TFQ^+_{RHS} + \alpha Q^+_{LS} \tag{5}$$

where F is the Fourier transform, T and D are the truncation and the horizontal diffusion, respectively. A reason for this is that α is a horizontally changing variable, so it cannot be moved before the horizontal operators.

The *t1* coupling changes the fields in the extension zone, so in the output the fields in the E zone differ from the large scale fields.

3. The tendency coupling scheme

We start from the following equation:

$$\frac{\partial Q_c}{\partial t} = (1-\alpha)\frac{\partial Q}{\partial t} + \alpha\frac{\partial Q_{LS}}{\partial t} \tag{6}$$

After discretisation (6) yields the following for 2TL scheme:

$$Q_c^+ = (1-\alpha)Q^+ + \alpha\left(Q^+_{LS} - Q^0_{LS} + Q^0\right) \tag{7}$$

Equation (7) differs from the flow relaxation scheme in the last two additional terms.

3.1 t1 version (not coded)

Originally it was planned to add the new terms to the t1 coupling scheme. In this case the scheme would be:

$$\left[(I-\beta\Delta tL)Q^+\right]_c = (1-\alpha)Q^+_{RHS} + \alpha(I-\beta\Delta tL)\left(Q^+_{LS} - Q^0_{LS} + Q^0\right) \tag{8}$$

As it can be seen in (8), the *(I - β∆t L)* operator should also be applied on $-Q^0_{LS}$ and Q^0. The problem with (8) is that only large scale variables have meaningful values in the extension zone. A solution could be to neglect $-Q^0_{LS} + Q^0$ there, but it is not sure then, that the coupled fields will be continuous. The reason for this is that Q^0_{LS} and Q^0 can differ even at the edge of the C+I zone due to the t1 coupling. Thus e.g. the Q^0 term in (8) should be biperiodicized, and although we only want to apply the scheme on the surface pressure, the biperiodicization would be costly in every time-step.

3.2 Splitted version (coded for 2TL with DM)

An other possibility is to place the additional terms to the beginning of the gridpoint calculations in the next time step. Thus this version consists of an original t1 coupling and a modification of the surface pressure and its derivatives at t0 level. In this case there is no need for the SI correction of the fields and the problem of the possible discontinuity disappears. The two steps are:

— *t1* coupling:

$$\left[(I-\beta\Delta tL)Q^{+}\right]_{c}=(1-\alpha)Q^{+}_{RHS}+\alpha(I-\beta\Delta tL)Q^{+}_{LS} \tag{9}$$

— *t0* level modification of the surface pressure in the next time step:

$$Ps_{c}^{0}=Ps^{0}+R\alpha\left(Ps^{9}-Ps_{LS}^{9}\right) \tag{10}$$

$$\left(\frac{\partial Ps^{0}}{\partial x}\right)_{c}=\frac{\partial Ps^{0}}{\partial x}+R\left[\alpha\left(\frac{\partial Ps^{9}}{\partial x}-\frac{\partial Ps_{LS}^{9}}{\partial x}\right)+\frac{\partial\alpha}{\partial x}\left(Ps^{9}-Ps_{LS}^{9}\right)\right] \tag{11}$$

$$\left(\frac{\partial Ps^{0}}{\partial y}\right)_{c}=\frac{\partial Ps^{0}}{\partial y}+R\left[\alpha\left(\frac{\partial Ps^{9}}{\partial y}-\frac{\partial Ps_{LS}^{9}}{\partial y}\right)+\frac{\partial\alpha}{\partial y}\left(Ps^{9}-Ps_{LS}^{9}\right)\right] \tag{12}$$

where Ps is the surface pressure and R is a multiplier aimed to stabilize the scheme, because experiments showed that it is unstable with R=1 . The reason for this is that due to the fact, that the t1 and *t0* coupling are not equivalent, the separation of the tendency coupling scheme can distort the scheme, as if other a coefficients were used for the separated terms in the coupling scheme and thus the chance of an instability is also larger.

4. Results

From the two aforementioned possibilities of the implementation of the tendency coupling scheme the splitted version was chosen to introduce into the ALADIN code by a new switch: LTENC. It was coded only for the 2TL scheme, so the experiments were only made on the hydrostatic model with SL2TL scheme. It was coded for both the quadratic and linear coupling, but there is a difference between them for technical reasons: for the quadratic coupling the tendency coupling is not applied at every NEFRCL step, only the original t1 coupling is done in these time steps. Although it breaks the ''continuity'' of the tendency coupling it did not seem to have any negative effect. For the linear coupling we put a new switch, LALLTC, that determines whether tendency coupling is applied in all steps or just t1 coupling in every NEFRCL steps. The multiplier *R* in (10-12) is called RTENC in the code and should be far enough below 1 to be stable, but close enough to 1 not to make a scheme, which differs from the original tendency coupling scheme very much.

4.1 2D experiments

The experiments were made on a linear hydrostatic flow over a 10m high Agnesi shaped obstacle. Most of them were started from and coupled with a perturbed surface pressure field by a 1hPa amplitude cosine wave, which had four wavelength in the C+I zone (first 180 points) and maximums at the edges of the C+I zone.

Figure 1 shows the vertical velocity when the surface pressure is perturbed. Now switching on the tendency coupling scheme (LTENC=. T.) with 10+1 identical LBC files, figure 2 shows the noisy results with a multiplier RTENC=1.0 for linear ''continuous'' tendency coupling (LALLTC=. T.).

Decreasing RTENC to 0.95 the noise disappears (Figure 3) and the field looks better in the coupling zone. Increasing RTENC above 1.0 the model can blow up, e.g. with RTENC=1.1 it blows up after 89 steps.

In the stable experiments the results with tendency coupling were better than those without it. A reason for getting good results was that the quality of the large scale tendency was better than that of the large scale field, i.e. the surface pressure perturbation was constant, so the large scale tendency was zero. An experiment was made to try a worse quality large scale tendency by using an opposite sign surface pressure perturbation in every second coupling file. The results were similarly bad for both the original t1 coupling (not shown) and the tendency coupling case with RTENC=0.9 (Figure 4). RTENC=0.95 gave noisy result in this experiment.

4.2 3D experiments

We ran the full model for only one case: the 1st of April 2001 on the LACE domain. For RTENC=1.0 the tendency coupling schemes seemed to be stable, at least I could not recognize any instability, and the verification results were sometimes better sometimes worse than that of the operational model. Although the previous case seemed to be stable we tried it with RTENC=0.9 to compare the accuracy. The verification results were similar, perhaps a little bit worse.

When RTENC=1.1 was set the model did not blow up, but the verification results were much worse. Of course one 3D experiment is only enough for a preliminary check, not for evaluation .

5. Modifications in the code

The tendency coupling scheme was coded only for 2TL scheme with DM. It is not coded for LSPLIT and B level parallelization, neither for NEDFI=6. The modifications of AL13 subroutines can be found in Prague in the directory sx4:/home/mma/mma142/AL13_tc.

6. Conclusion

The interpolation of the surface pressure from the large scale model's orography to the nested model's one can cause imbalance in the surface pressure field. This can result in the coupling of the unbalanced pressure. To decrease this harmful effect we applied a tendency coupling scheme for the surface pressure. It consists of a t1 coupling and a modification of the surface pressure and its derivatives at t0 level. This scheme proved to be unstable in 2D experiments probably due to the splitting of it, but a simple modification of the scheme made it stable. The results of the 2D experiments are better with tendency coupling, when the surface pressure is perturbed and has constant value in time in the LBC files. When the surface pressure perturbation changes sign in every next LBC file the results of the tendency coupling scheme are similarly bad as those of the original t1 coupling scheme. A 3D experiment shows that the quality of the forecast with the tendency coupling scheme is probably similar to that of the operational model. The tendency coupling scheme was coded for the 2TL scheme and DM, the newest version of the modified subroutines of AL13 can be found in Prague in the directory sx4:/home/mma/mma142/AL13_tc.

References

P. Bénard (1999), Scientific documentation for ALADIN NH model

M. Janisková (1994), Study of coupling problem

G. Radnóti (1995), Comments on ''A spectral limited-area formulation with time-dependent boundary conditions applied to the shallow-water equations'', MWR, Vol. 123, 3122-3123.

T. Szabó (2001), Tendency coupling of the surface pressure and related modifications in the code, Prague report

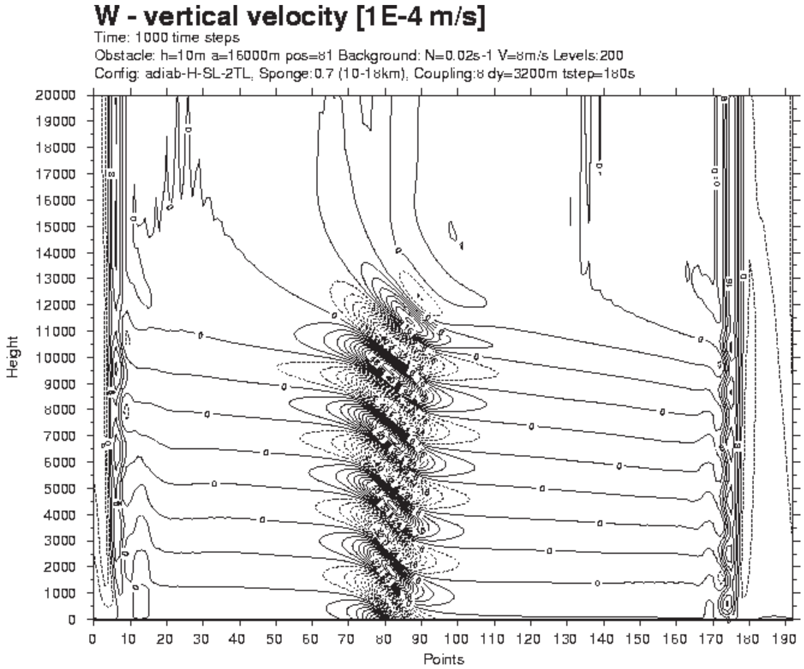

Figure 2: Result without tendency coupling when the surface pressure is perturbed artificially in the coupling files

Figure 1: Result without tendency coupling when the surface pressure is perturbed artificially in the coupling files

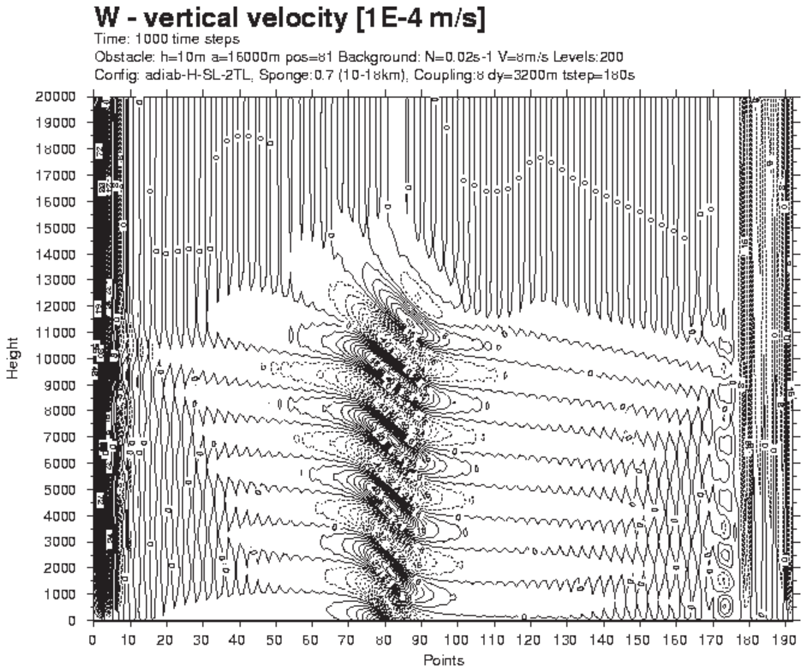

Figure 4: Result with linear continuous tendency coupling and surface pressure perturbation. RTENC=1.0

Figure 2: Result with linear continuous tendency coupling and surface pressure perturbation. RTENC=1.0

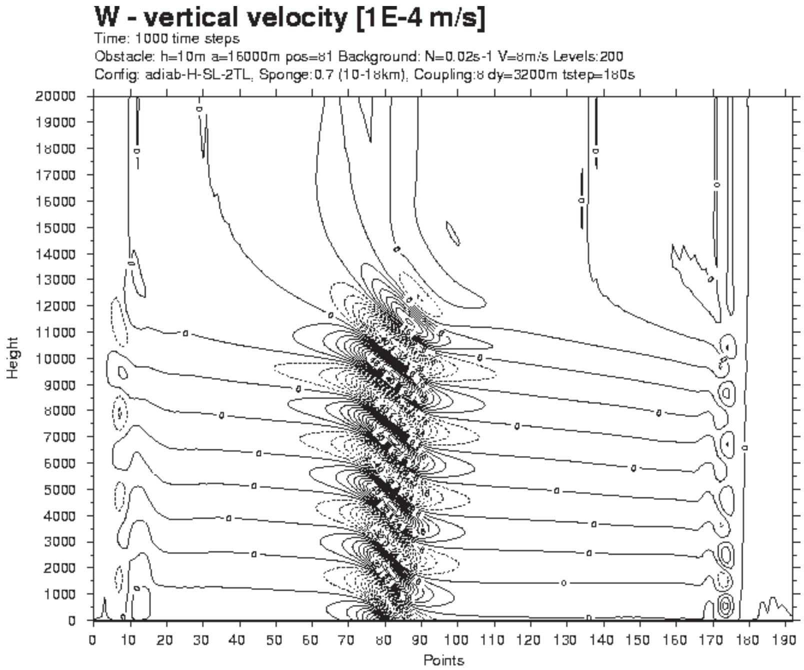

Figure 3: Result with linear continuous tendency coupling and surface pressure perturbation. RTENC=0.95

Figure 3: Result with linear continuous tendency coupling and surface pressure perturbation. RTENC=0.95

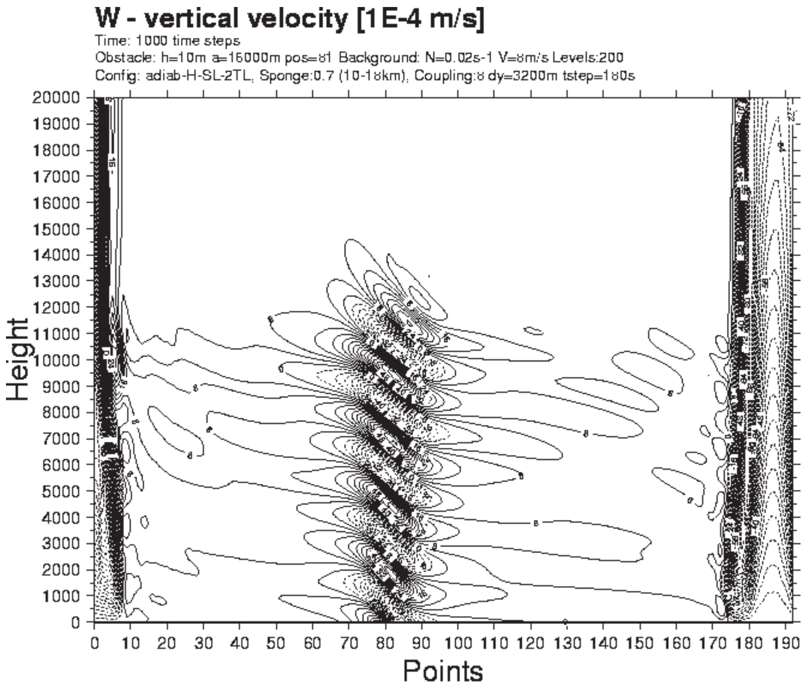

Figure 9: Result with opposite sign surface pressure perturbation in every second lbc file, with linear continuous tendency coupling and RTENC=0.9

Figure 4: Result with opposite sign surface pressure perturbation in every second LBC file, with linear continuous tendency coupling and RTENC=0.9

A summary of the latest changes in the parameterization of turbulent fluxes and PBL processes

Jean-François Geleyn, September 2001

Introduction

The surface and atmospheric turbulent exchange schemes are designed in continuity following the suggestion of *Louis* (1979). However the exact implementation of the basic algorithms is the one suggested in *Louis et al.* (1982) where a few additional "physical" constraints are put on the formulation and the interdependence of constants. Hence, apart from the rather arbitrary prescription of the asymptotic mixing lengths for momentum and temperature/moisture four "historical" constants always controlled the intensity of vertical exchanges and their functional dependency on stability:

- κ : von Karman constant ;
- b : the slope of the Monin-Obukhov universal function for momentum at neutrality ;
- c : a free-convection limit adimensionalised constant ;
- d : a non-dimensional constant representing the divergence of the momentum and heat functions in the stable case, linked to the maximum flux Richardson number in the stable case.

The current names and tunings for these constants are :

$$\kappa = VKARMN = 0.4\ ,\ \ b = EDB = 5.\ ,\ \ c = EDC = 5.\ ,\ \ d = EDD = 5.$$

The studies performed along the last two years resulted in a concerted reformulation of the vertical profiles of mixing lengths and the model representation of the effective Richardson number for stable cases, together with the correction of some inconsistencies in the management of momentum versus heat fluxes.

Description of mixing and roughness lengths

The prescription of the asymptotic mixing lengths for momentum (M) and heat (H) required several adjustments and it was found that a functional representation with 3 parameters for each of the two cases was necessary. The 3 parameters are the asymptotic mixing lengths respectively at top and bottom of the atmosphere (or rather the bottom one λ and their ratio β) and a "transition height" H, the formula for the mixing lengths themselves finally being :

$$l_{M/H}(z) = \left(\beta_{M/H} + \frac{1-\beta_{M/H}}{1+\left[\frac{z+z_{0,M/H}}{H_{M/H}}\right]^2} \right) \cdot \left(\frac{1}{\kappa \cdot (z+z_{0,M/H})} + \frac{1}{\lambda_{M/H}} \right)^{-1}$$

l increases from the ground ($l \approx \kappa z_0$ as $z \to 0$) up to $l \approx \lambda /2.5$ at $z \approx H/2$, then decreases towards $l \approx \beta\lambda$ as $z \to \infty$.

The number of independent parameters is in fact smaller, reduced to 3 through the relationships :

$$\lambda_H = \lambda_M \cdot \frac{3}{2} d \qquad \beta_H = \beta_M / \sqrt{3} \qquad H_H = H_M \cdot \sqrt{3}$$

The current names and tunings for these independent parameters are :

$$\lambda_M = ALMAV = 300 \text{ m}, \ \beta_M = BEDIFV = 0.05 \text{ and } H_M = UHDIFV^{-1} = 1250 \text{ m} .$$

The main changes, still in test in September 2001 (CYCORA-ter parallel suite), are :

- changes of the ratios λ_H / λ_M and β_H / β_M , now chosen according to the asymptotic behaviour as $z \to \infty$;
- improved consistency in the definition of l_H, now depending on $z_{0,H}$ instead of $z_{0,M}$.

This consistency also modifies the exchange coefficients : $K_H = l_M \, l_H \, f_H(...)$ and $K_M = l_M{}^2 \, f_M(...)$. The figure hereafter shows the old (dashed lines) and new (full lines) profiles of l_M (blue), l_H (red), and the effective length now used in the exchange coefficient for heat : $\sqrt{(l_M l_H)}$ (purple).

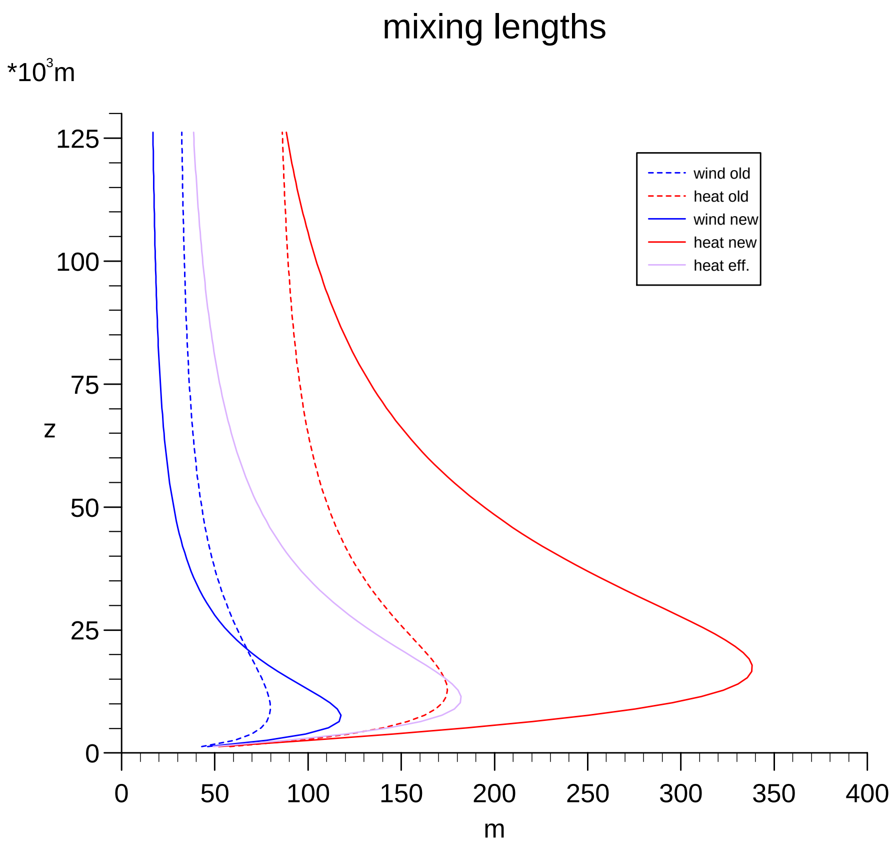

No change was introduced recently concerning roughness lengths. Values over land are constant, derived from orography, urbanisation and vegetation cover. The ratio z_{0H}/z_{0M} has been tuned to .10 here. Over sea we are however using the so-called Charnock formula with and additional "gustiness" stability dependent term. The latter has been introduced to ensure that, in low wind and unstable conditions the heat fluxes do not drop to zero, not for lack of a correct formula (the limit case is in principle taken into account by the Louis scheme), but simply for a vanishing roughness. Thus the formula now reads :

$$z_{0,M} = z_{0,H} = C_{hk} \cdot u_*^2 / g \ + \ z_{0,cr} C_D \ / C_{DN}$$

where :

- C_{hk} is the Charnock constant (*VCHRNK*), currently set to 0.021 ;
- $z_{0,cr}$ is the critical "low wind" neutral roughness length (*VZ0CM*), set to 1.5 10^{-4} m ;
- u_* is the friction velocity, computed from the wind at the lowest model level as : $u_*^2 = u_L^2 \times C_D$;
- C_D and C_{DN} are respectively the drag coefficient and its neutral counterpart .

We are currently investigating the possibility to replace this formula by another one in the case of moist convective activity, with a progressive transition between the two extremes of "dry" and "moist" gustiness.

Description of the Richardson number

The formulation of Ri^*, the "effective" Richardson number used in computations for the stable case instead of the initial one Ri, is far more complicated now, with differences between the values used for heat and momentum fluxes.

The former parameterization of the vertical turbulent fluxes in the stable case (both at the surface and in the atmosphere) included a limitation of the Richardson number to a value Ri^{cr} which inverse was named *USURIC* in the code. It was introduced in May 1997 to avoid the negative feedback of the reinforcement of stability in the case of very cold surface, i.e. simulating the fact that less stable parts of an inhomogeneous flow always dominate the vertical flux computations owing to the strong nonlinearity of the fluxes with respect to the gradient of potential temperature. In practice the employed equation was trivially simple :

$$Ri^* = Ri \ / [1 + \frac{Ri}{Ri^{cr}} \ ]$$

The new formulation reads :

$$Ri^*_{M/H} = Ri \ \ /[1 + \alpha_{M/H}(Ri,z) \cdot \frac{Ri}{Ri^{cr}(z)} \ ]^{\ \alpha_{M/H}(\mathrm{Ri},z)^{-1}}$$

A first new development consisted in replacing Ri^{cr} by Ri^{cr}/U_{cl} at the surface and designing a vertically varying profile between the top of the atmosphere (where Ri^{cr} keeps its original value) and the bottom part of the PBL (where it tends towards the new surface value). This moved to operations in October 1999, with the first CYCORA package. The chosen expression for this variation is controlled by an exponent U_{ce} :

$$Ri^{cr}(z) = Ri^{cr}_{\infty} \ / \ \left(1 + (U_{cl} - 1)[\ \frac{l_H(z)}{\kappa \cdot (z + z_{0,H})} \ ]^{U_{ce}}\right)$$

The former variable *USURIC* is now the inverse critical Richardson number at infinity, set to 1. , while U_{cl} =*USURICL* = 4. and U_{ce} =*USURICE* = 0.5 .

Next, the tests carried out on the 1998 and 1999 storm cases, which have shown a very strong sensitivity to the values of the exchange coefficients in stable regime, led to enlarging the usage of the critical Richardson number through a scaling factor α, differing for heat and momentum. The new formulation is more general and has the same behaviour near the neutral state. But for $\alpha > 1$, in the very stable cases, the exchange coefficients tend towards zero as it was the case in the operational situation before May 1997 ($Ri^{cr} \equiv 0$). Theoretical considerations (and related computations) have shown that the values :

$$\alpha_M = 1 \text{ (for momentum) and } \alpha_H = 3 \text{ (for temperature and humidity),}$$

have the desired properties, i.e. an asymptotic value of the sensible heat flux and a convergent critical Richardson flux number, irrespective of the Ri^{cr} value, as $Ri \rightarrow \infty$.

Due to the little influence of α near the neutrality it might have been sufficient to have a unique value for each of the two types of coefficients. Unfortunately no compromise is possible in this case and the positive effect of strong values of $1/Ri^{cr}$ for a realistic behaviour of the storms is systematically lost. To solve the problem a second transition was introduced for heat (temperature and humidity) :

$$\alpha_H = \frac{3Ri + Ri^d(z)}{Ri + Ri^d(z)}$$

, where Ri^d is a new tunable "parameter", while for momentum the "status quo" was kept :

$$\alpha_M \equiv 1.$$

In fact the above approach has only changed the state of the problem : a realistic simulation of the storm activity requires big values of Ri^d (~100 or even more) while to avoid the inversion erosion small values of Ri^d (around 10 or less) are necessary. The results of the experiments, showing values of Ri^d controlling the storm development at the top of PBL and inversion erosion near the surface, led to the introduction of a vertical variation for Ri^d too. Its vertical profile is determined by the asymptotic value in the upper atmosphere and an exponent characterizing the vertical variation :

$$Ri^d(z) = Ri^d_{TOP} / \left(1 + \frac{H_M \cdot H_H}{(z + z_{0,M}) \cdot (z + z_{0,H})}\right)^{U_{de}}$$

Ri^d at the top of the atmosphere (*USURID* $^{-1}$) is tuned to about 30 and U_{de} (*USURIDE*) to 1 . At the surface Ri^d is taken to 0.

The figure hereafter shows the vertical profiles of the intermediate Ri^{cr}, Ri^d and Ri^* quantities, for a constant vertical profile of Ri ($Ri \equiv 10.$).

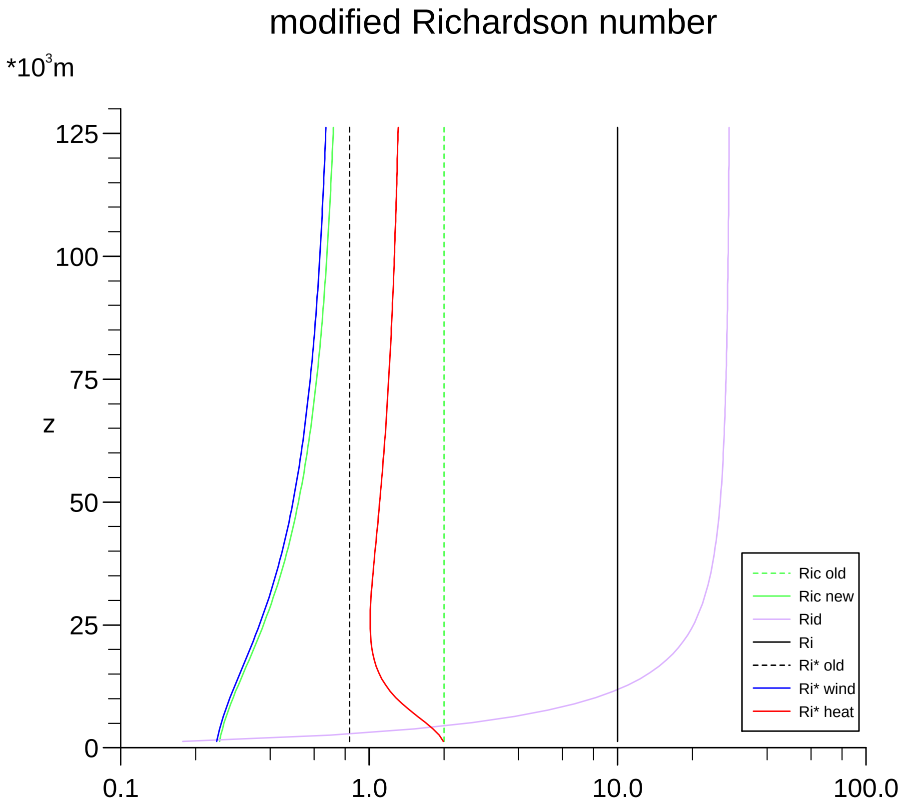

Antifibrillation scheme

The scheme, described in details in *Bénard et al.* (2000), was updated consistently.

References

Bénard P., A. Marki, P.N. Neytchev and M.T. Prtenjak : Stabilisation of non-linear vertical diffusion schemes in the context of NWP models. *Mon. Wea. Rev.,* vol. 128 n° 6, pp. 1937-1948.

Louis, J.F., 1979 : A parametric model of vertical eddy fluxes in the atmosphere. *Bound.-Layer Meteor.*, **17**, 197-202.

Louis, J.F., M. Tiedke and J.F. Geleyn, 1982 : A short history of the operational PBL parameterization at ECMWF. *Workshop on planetary boundary layer parameterization*, ECMWF, 25-27 nov 1981, pp 59-80.

and

Bellus, M., 2000 : Vertical turbulent transport parameterization (the vertical profile for USURID parameter)

Belo Pereira, M., 2000 : Diagnostic of the shape of the exchange coefficients used in vertical diffusion

Gérard, L., 2000. : Documentation of physical parameterizations - Part III : Turbulent fluxes and PBL processes. (to be updated)

Simon, A., 2001 : Horizontal and vertical diffusion parameters tests on ARPEGE and ALADIN on problematic situations.

Scores of ALADIN-FRANCE during the first semester of 2000

(more details : francis.pouponneau@meteo.fr or samuel.westrelin@ meteo.fr)

1. COMMENTS OF SCORES AGAINST SYNOP - FIRST SEMESTER 2001

The scores (bias and root mean square error) plotted on the next figures are calculated against SYNOP over the whole domain ALADIN-FRANCE. Scores are averaged over the first semester 2001.

They use about 200 synoptic stations over the domain.

MSLP
The RMS rises with forecast range from 0.6 to 2.3 hPa. The model underestimates this parameter from 12 hours range till 48 hours to reach -1. hPa.

CORRECTED TEMPERATURE
We can see a diurnal cycle of the bias (overestimated at 12 UTC validity time - forecast ranges 12 and 36 hours - at maximum 0.5°K and underestimated during night at maximum -0.7°K) which is on average -0.5°K.

WIND INTENSITY
Its RMS is quite stable with ranges. It is not biased on night but clearly underestimated on afternoon. The mean bias over ranges is about -0.3 m/s.

2. COMMENTS OF CONTINGENCY TABLE - FIRST SEMESTER 2001

Tables below are the cloud cover and precipitation contingency tables for ALADIN-FRANCE 36 hours forecast range. Units are octas for cloud cover and mm/6 hours for precipitations.

We present several contingency indexes :

-pnd : probability of no detection

-far : false alarm rate

-pod : probability of detection

-fbi : frequency bias index (the closer to 1 the better)

-ts : threat score (the closer to 1 the better)

-tss : true skill statistics (the closer to 1 the better)

They are computed for different thresholds. It gives the model skill to detect phenomenons over each threshold. For example, considering the threshold 3-6 for cloud cover, a two by two contingency table is rebuilt with one class mixing classes 3-6 and 7-8 (phenomenons whose intensity is equal or higher than the threshold) and another class being the 0-2 class. Indexes are computed over this new table.

CLOUD COVER

For threshold "3-6", pod is 84% and far very low, 8%. But with increasing threshold, pod drops to 42% (less than one event over two is detected) and far rises to 22%.

PRECIPITATIONS

Threshold "0.1-2" measures the model ability to discriminate the rain/no rain events. far is high (when rain is forecast, on 44 cases over 100 it does not rain) but this is at least partly due to a bias in the methodology (rain gauge measurement compared to the nearest model grid point) because we compare what is representative of the model scale (mesh size, about 100 square km) to a rain gauge (representative of a few square meters). pod is 72%.

Considering increasing thresholds, which correspond to more severe meteorological events, the quality of the indexes falls dramatically. For "10 and more" threshold, far is 79% and pod, very poor, 22%.

Note that the model can be climatologically well tuned (fbi very close to 1 for "2-10" and "10-more" thresholds) but it does not mean it gives the right amount of precipitations at the right place and time.

3. SCORES AGAINST SYNOP - FIRST SEMESTER 2001

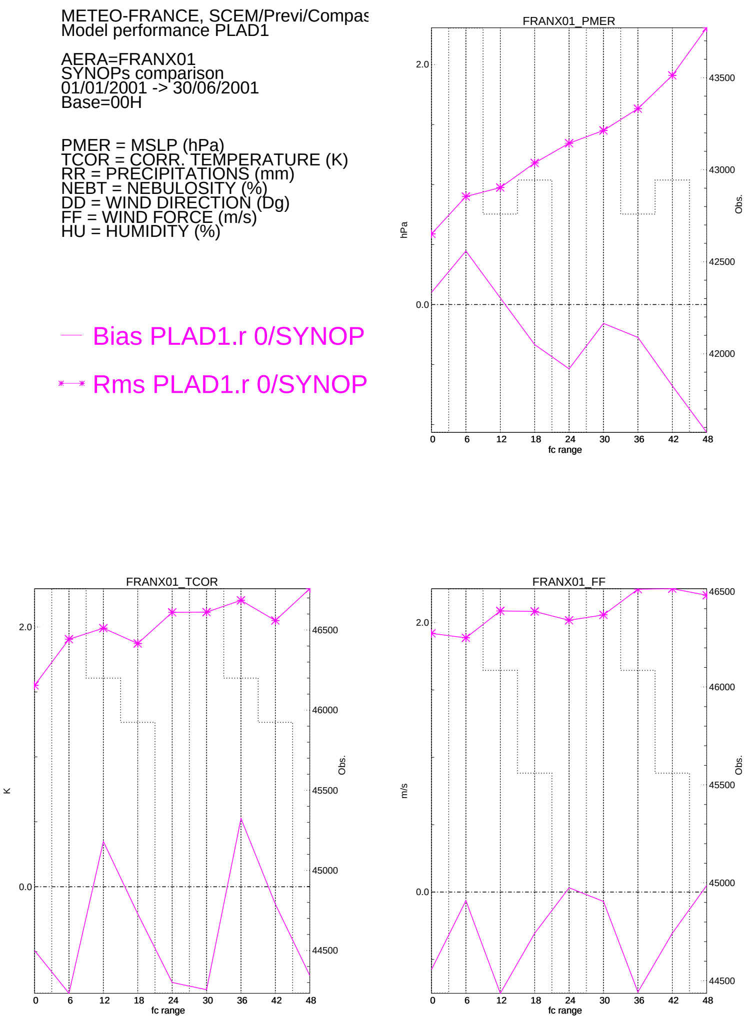

4. CONTINGENCY TABLE - FIRST SEMESTER 2001

Period: 200101 - 200106

Cloud cover Aladin, Synoptic time:00, Range:36 H

Obs/Forecast	0-2	3-6	7-8	Total
0-2	**11.9%**	5.3%	0.3%	17.6%
3-6	9.1%	**18.6%**	5.5%	33.3%
7-8	4.3%	24.3%	**20.6%**	49.1%
Total	25.3%	48.2%	26.4%	**42103**

Contingency Indexes

Threshold	pnd	far	pod	fbi	ts	tss
3-6	0.16	0.08	0.84	0.91	0.78	0.52
7-8	0.58	0.22	0.42	0.54	0.37	0.30

Precipitation Aladin, Synoptic Time:00, Range:36 H

OBS/Forecast	No rain	0.1-2	2-10	10-	Total
No rain	**58.4%**	12.7%	2.1%	0.2%	73.4%
0.1-2	5.6%	**7.5%**	2.9%	0.2%	16.3%
2-10	1.6%	3.7%	**3.6%**	0.4%	9.4%
10-	0.1%	0.2%	0.4%	**0.2%**	0.9%
Total	65.8%	24.2%	9.1%	1.0%	**45546**

Contingency Indexes

Thresold	pnd	far	pod	fbi	ts	tss
0.1-2	0.28	0.44	0.72	1.28	0.46	0.52
2-10	0.55	0.53	0.45	0.97	0.30	0.39
10-	0.78	0.79	0.22	1.03	0.12	0.21

ALATNET developments during the first half of 2001 in the ALATNET centers

1. In Toulouse (France)

The work of the two ALATNET PhD students in Toulouse, Gianpaolo Balsamo and Cornel Soci, is described in separate reports. The summary hereafter corresponds to the joint efforts of the other visitors and the permanent staff.

1. <u>Theoretical aspects of non-hydrostatism (NH)</u>

Significant progress was obtained concerning the stability of semi-implicit semi-Lagrangian advection schemes in NH dynamics. An overview of the latest results from the Toulouse [T] and Prague [P] teams is available in the proceedings of the 10th ALADIN workshop : "*Progresses in NH numerics*", by Pierre Bénard [T] , Radmila Brozkova [T,P], Jozef Vivoda [P] , Christopher Smith [P] , Petra Smolikova [T] , and Jan Masek [T] .

4. <u>Removal of the thin layer hypothesis</u>

The current state of research is described in the proceedings of the 10th ALADIN workshop : "*Relaxation of thin layer hypothesis in the model ARPEGE / IFS : application to Eulerian scheme*", by Karim Yessad. Abdelwaheb Nmiri began to examine the specific ALADIN features during its stay.

5. <u>Coupling and high resolution modes</u> & 6. <u>Specific coupling problems</u> (6b: Tendency coupling for surface pressure and other technical variations around Davies' technique of field coupling in a buffer zone)

Jean-Marc Audoin has just joined the small team working on coupling problems : Gábor Radnóti, Tamás Szabó and Piet Termonia. In consequence the main effort during this six months consisted in discussions with Piet Termonia and Gábor Radnóti during their stays in Toulouse, and collecting/reading documentation.

6. <u>Specific coupling problems</u> (6a: Blending of fields in data assimilation for preserving high resolution forecast details)

The "blending" test-suite for ALADIN-France was refined (Olivier Pédoussaut, Adam Dziedzic, Claude Fischer) and some sensitivity experiments performed, as described in he proceedings of the

10th ALADIN workshop : "*DFI-Blending dans le modèle ALADIN/France, étude d'impact des filtres digitaux*", by Adam Dziedzic. A detailed documentation was written by Dominique Giard, starting from the sparse previous reports, and is available via the ALATNET and ALADIN web sites.

8. Adaptation of physics to higher resolution (8b: Test, retuning and improvement of the various physical parameterisation in the framework of a very high resolution)

Till the first "CYCORA" package (autumn 1999), the problem of the horizontal resolution dependency of the convection scheme, i.e. the partition between resolved and unresolved precipitations, was partially cured, following the results of Jean-Marcel Piriou (1991), by introducing a modulation of the dynamical part of the humidity convergence by a factor depending on the model resolution. Afterwards the stratiform or resolved precipitations were computed first and then the humidity convergence available for convection was reduced correspondingly, in order to avoid a double count. However recent studies, mainly :

- the work of Frédéric Sourgen concerning the skill of ALADIN for the prediction of tropical cyclones,
- the work of Doina Banciu in Romania, described in a specific paper in the proceedings of the 10th ALADIN workshop : "*Simulation of the mesoscale convective systems at different resolutions*",

showed severe inconsistencies. "Stratiform/resolved" precipitations decreased and "convective/ unresolved" ones increased as the mesh-size was reduced.
A mixed solution with a lowering of the transition scale from 17 to 10km was tested on a wide set of situations and will be part of the "CYCORA-ter" package, to be tested in a parallel suite next autumn. Let us recall that CYCORA is an alias for CYclogenis + COnvection + RAdiation.

8. Adaptation of physics to higher resolution (8c: Improved representation of boundary layer)

André Simon, with some help from Jean-François Geleyn and Jean Pailleux, analysed the reasons of the exaggerated cyclonic activity in ARPEGE (and ALADIN, indirectly) mainly over sea and at fine scales. The study rapidly evolved towards considerations of increased mixing length for the turbulent vertical diffusion parameterisation scheme. A lot of different solutions were tested, including retuning of the most crucial parameter of the CYCORA-bis package (Ri_d, related to the modified formulation of the Richardson number), in order not to lose benefits of past work on the 1998 and 1999 Christmas' storms. The proposal, put in a temporary parallel suite, was excellent for the surface part of the problem, with a better structure of pressure lows. But its too simple character (proportional increase of mixing length everywhere) led to strong degradations at the tropopause level and around, where fields were over-smoothed. He addressed afterwards the (sometimes really old) problems of consistency in the definition of the mixing lengths for heat and momentum (computation and respective usage). This study was pursued by Jean-Marcel Piriou, Eric Bazile and Jean-François Geleyn. After intensive validations, a new set of modifications, with different tunings for heat and momentum, is ready to enter "CYCORA-ter".

8. Adaptation of physics to higher resolution (8d: Improved representation of orographic effects)

Steluta Alexandru designed new formulations for the two cost functions used in the computation of spectral orography for ALADIN. The fraction of sea is now taken into account, not only the height, so as to better preserve contrasts along coasts. A summary of her work is available in the proceedings of the 10th ALADIN workshop : "*Tuning the orography representation in the E923 configuration*", by Steluta Alexandru. This work also gave the opportunity to correct a very old bug, as old as E923 : the height values in the extension zone where taken into account in the cost function, though meaningless. The two formulations were also harmonized, to make further tuning easier.

9. Design of new physical parameterisations (9b: Use of liquid water and ice as prognostic variables, implementation of a new microphysics parameterisation)

A modular approach for the parameterization of moist processes, the so-called "Functional Boxes", is under study for some years. It must :

- handle the vapour, liquid and ice phases of atmospheric water,
- allow to test independently various parameterizations for convection, microphysics, ...
- be portable to other NWP models.

A first version is now available and was tested in the 1d version of ARPEGE/ALADIN, using GATE observations. Results are promising. This work was presented at the 10th ALADIN workshop and the corresponding paper is available on the ALATNET and ALADIN web sites *: " "Functional Boxes" approach for moist processes* ", by Eric Bazile.

9. Design of new physical parameterisations (9c: New parameterisation of exchanges at sea and lake surface)

Taking advantage of the short stay of Mihaela Caian in Toulouse, a closer collaboration between the French and Romanian teams was organized and a new experimental framework designed to evaluate the impact of a parameterization of lakes.

9. Design of new physical parameterisations (9d: Improved representation of land surface, including the impact of vegetation and snow)

Discussions with Mihaela Caian also led to new proposals for a simple description of the impact of urbanisation within the current land surface scheme. However this cannot be tested before the new, high resolution, land-cover map is fully available. And significant modifications were brought to this database till June, delaying its adaptation to the ARPEGE/ALADIN framework.

The work on snow cover progressed in two directions. First Mohamed El Haiti and Eric Bazile refined the previous modifications, i.e. introducing the albedo of snow as a new prognostic variable and taking into account the vegetation (coverage, leaf area index, albedo) in the formulation of the snow coverage and the global surface albedo. The age of snow, estimated from the albedo, is now considered in the definition of the snow fraction, and a saturation of the dependency on the leaf area index is introduced. However some more retuning, e.g. of the formulation of thermal inertia, and more extensive sensitivity experiments are required. Second a simplified version of this new scheme contributed to the international SNOWMIP experiment, for the intercomparison of snow-cover parameterizations, and proved as good as several more sophisticated schemes.

9. Design of new physical parameterisations (9e: Refinements in the parameterisations of radiation and cloudiness)

Janko Merse tried to solve the problem of the underestimation of cloudiness below very stable layers using the data produced by a cloud-resolving model (CRM) as the basis for validation. This study is described in : "*Relations between water particles content, vertical stability and cloudiness in cloud resolving models*", published in the proceedings of the 10th ALADIN workshop. But it failed because of a conceptual problem in the CRM used here.

10. Use of new observations (10a: Yet unused SYNOP observations) : see the ALADIN report

10. Use of new observations (10b, 10d : satellite observations)

As a preliminary to the use of new satellite data at high resolution over continental domains, Malgorzata Szczech began to implement a more detailed description of surface emissivity in the model, with dependency on vegetation, season, and wavelength, and consistent with the model land cover. A more detailed paper is available in the proceedings of the 10th ALADIN workshop : "*Improved description of emissivity over land*".

Roger Randriamampianina got an intensive training on the treatment and the use of satellite data, analysing the impact of local ATOVS observations, available sooner and at higher resolution over France, on short-range forecasts over Europe.

Thanks to Philippe Caille, new types of observations are now routinely pre-processed and available to modellers. The impact of some of them was studied along the last months, but in a global framework. A summary is available on the ALATNET and ALADIN web sites : "*Use of ATOVS and SSMI observations at Météo-France*", by Florence Rabier, Elisabeth Gérard, Zahra Sahlaoui, Mohamed Dahoui and Roger Randriamampianina.

11. 3D-Var analysis and variational applications (11a: Definition and calculation of new background error statistics, impact of domain resolution and extension, identification of horizontal relevant scales)

Mohamed Raouindi examined, with Loïk Berre, the basic homogeneity hypothesis used in the computation of background error statistics for ALADIN up to now, so as to keep only diagonal terms. He exhibited a latitudinal dependency of spatial covariances for ALADIN-Maroc : thinner vertical structures and wider horizontal ones as the latitude decreases. Sensitivity experiments indicated the possibility to select some important couples of meridional wavenumbers to be related to each other (using a block-diagonal covariance matrix), in order to represent the identified latitudinal variability in an economical way.

11. 3D-Var analysis and variational applications (11b: Scientific investigation of the problem of the extension and coupling zone, analysis of the impact of initialization)

A detailed study of the respective impacts of 3d-var analysis and digital filter initialization on spectral fields in ALADIN was performed by Simona Stefanescu. She compared large-scale versus mesoscale background error statistics for 3d-var, with varying weights for the differents parts of the cost-function, and incremental versus full versus no initialization. Her main conclusions are : initialization should be used incrementally, its impact is noticeable at the smallest scales and sensitive to the weight of vorticity in the background cost function, and coupling is a significant source of noise.

11. 3D-Var analysis and variational applications (11c: Management of observations in 3d-var)

Wafaa Sadiki and Sandor Kertesz studied how to adapt the operational selection of observations to the case of a high-resolution limited-area model.

11. 3D-Var analysis and variational applications (11f: Development of variational type applications (adjoint methods for sensitivity studies, singular vectors), as a project itself and to provide more insight into the coupling problem for 4d-Var)

The configuration 601, adapted to ALADIN and carefully updated for several years by Claude Fischer, produced its first results last spring under the hands of two French students, Vincent Guidard and Pierre-Luc Payet. It uses a Lanczos algorithm to produce the first singular vectors of the model, i.e. the most unstable perturbations of the initial conditions, for a given time-span and a given situation. It was run for large ALADIN domains at a low resolution (30 km) and at the full ALADIN resolution (10km) for small targeted areas. The identified structures look quite sensible at first. Some examples may be found in the devoted paper : "*Singular vectors in ALADIN*", by Claude Fischer, Vincent Guidard and Pierre-Luc Payet, in the proceedings of the 10th ALADIN workshop. More details may be asked to Claude Fischer.

12. 4D-Var assimilation (12d: Improvement of the treatment of humidity in data assimilation)

The problem noticed in the management of humidity by 4d-var assimilation in ARPEGE was identified and temporarily solved. More details may be found in the report from Radi Ajjaji.

2. *In Bruxelles (Belgium)*

RMI

5. Coupling and high resolution modes

A description of the corresponding work is available in the proceedings of the 10th ALADIN workshop : "*Tests of some temporal interpolation schemes for the coupling mechanism*", by Piet Termonia.

6. Specific coupling problems (6a: Blending of fields in data assimilation for preserving high resolution forecast details)

Alex Deckmyn designed a test blending suite for ALADIN-Belgium

8. Adaptation of physics to higher resolution (8a: Parameterisation of the small-scale features of convection)

A summary of the corresponding work is available in the proceedings of the 10th ALADIN workshop : "*Some results using a prognostic convection scheme in ARPEGE-ALADIN*", by Luc Gérard.

8. Adaptation of physics to higher resolution (8d: Improved representation of orographic effects)

Philippe Nomerange started analysing the representation of the small-scale orography features in ALADIN. After a bibliographic research phase aimed at learning and understanding the various methods that can be used to represent the small-scale effects of the orography - envelope orography, improved roughness length, ... - a comparison phase between those methods has been started using a test case of ALADIN on a domain covering the Pyrénées.

3. *In Prague (Czech Republic)*

1. Theoretical aspects of non-hydrostatism

1a) Top and bottom boundary conditions *(C. Smith)*

When making the experiments with the so-called non-hydrostatic nonlinear regime (in 2d vertical plane), we noticed that in case of the semi-Lagrangian advection treatment there is a small spurious standing wave above the mountain. This spurious pattern does not appear when using the Eulerian scheme. In fact, it is sufficient to have relatively high mountain and some mean flow to reproduce the spurious pattern. A defect of this type occur even in case of the potential flow regime. In order to find the cause, the semi-Lagrangian discretisation was examined especially for the 3d continuity equation (treatment of the 3d divergence) and for the bottom boundary condition. The spurious patterns depends on the length of the time-step, though it is not very clear at this stage whether it has to do something with the length of trajectory or not. At the moment the influence of the individual terms in the equations on the spurious pattern is investigated. There are also a few ideas how to improve the current discretisation of the bottom boundary condition.

1b) Predictor-corrector scheme *(J. Vivoda)*

The predictor-corrector scheme for the 2TL non-hydrostatic semi-Lagrangian scheme is basically working. However, in presence of a steep orography 3 iterations of the scheme are necessary in order to obtain a stable integration. This is in contradiction with the linear stability analysis results where only one iteration of the scheme would have been fully sufficient. To understand this result, one has to keep in mind that the basic linear stability analysis does not evaluate the effects of purely nonlinear terms. For example, one part of the 3d divergence linked to the coordinate transformation from z to η and denoted as X is not evaluated (the term X is equal to "$\partial V / \partial \varphi$ dot grad(φ)", hence closely depending on the orography gradient). There are all reasons to think that the term X is responsible for the instability linked to the orography: an enhanced linear stability analysis taking into account this term by introducing a constant orographic slope over the domain showed the instability (as demonstrated by Pierre Bénard). However results of the enhanced analysis has to be taken with some precautions since the constant slope does not fulfil the periodic condition, for example.

During the successive corrector steps the semi-Lagrangian trajectories can be recomputed to achieve higher accuracy. It was expected that improved accuracy will accelerate the rate of convergence and thus minimise the number of needed iterations. The following methods of trajectories re-computations were tested: i) first and second order accuracy approximation during the predictor step followed using the second order approximation during the corrector steps; ii) the second order approximation was used in the predictor step and the third order approximation was used in the corrector step. It was experimentally found that these trajectory re-computations have not improved the speed of convergence.

2. High resolution runs

2.a) Experimental framework *(D. Cemas)*

Thanks to the availability of the ee923 configuration (Jure Jerman) the 1km mesh-size domain with sufficiently fine orography was created. Hence, the very first tests of ALADIN on 1km domain are ready to start this summer. These tests are meant to discover the major difficulties to run the model on such a mesh. The domain includes a very sharp orography (the Julian Alps) and will serve for benchmarking ALADIN NH versions as they will evolve.

2.b) Lipschwitz versus CFL criteria *(Alena Trojakova, Radmila Brozkova)*

The study of the applicability of Semi-Lagrangian schemes in NWP models with respect to the dependency on the increase of spatial resolution of the computational grid shall be based on the pseudo-academic SCANIA-type of tests. The model will be launched at finer and finer resolution, going from 10km to 156m horizontally and from 867m (30 levels) to 108m (240 levels) vertically, by keeping the same depth of the atmosphere. The specially prepared fine mesh orography from the Alpine region shall be used (with help of CNRM/GMME). However, the nesting of domains requires a procedure of the EE927-type in order to prepare the initial and lateral boundary conditions for each inner domain. Here the standard Full-Pos approach does not satisfy the specific academic conditions, therefore a simple procedure is currently being developed and validated, using only the core interpolating routines (*HORIBLE, APACHE*). This academic procedure may be also useful in future for any kind of similar needs.

3. Data assimilation related coupling issues

3.a) The blending technique operational in ALADIN/LACE *(F. Vana, M. Siroka, D. Klaric)*

Starting from 6th June 2001, the ALADIN/LACE initial conditions are computed using the blending technique instead of a pure dynamical adaptation method. The first operational version of the blending algorithm comprises the treatment of both spectral and surface fields. The tuning was retained as established during the period of the extensive testing: The cut-off spectral truncation represents the mesh of about 30 km, the internal digital filters work with the stop-band edge of 5 hours and there is no external initialization within the long cut-off cycling procedure. Only a weak external digital filter with the stop-band edge of 1 hour and a half is applied in the 48 hour production forecasts. the blending of the surface fields, these are blended only over the land surface (the sea points are left without any change). The cycling procedure is fully in phase with the data assimilation cycle of ARPEGE, at least for what concerns the long cut-off cycle. The production blending and following forecasts are done only twice a day for the time being. Within the spring 2001, the blending algorithm was phased with the operational library AL12_op6 and the source code was cleaned. In May, a bug in the handling of the surface monthly constants was discovered and corrected (see also the Prague Team short report in the ALADIN Newsletter). The last validation tests before the operational application of the blending technique were done at the end of May, beginning of June. The next research and development work using the blending algorithm is scheduled for July 2001, where the incremental digital filter initialization should replace the remaining external initialization in the production forecasts. The combination of the blending technique with the linear grid (higher spectral resolution) will also be a R & D topic in the second half of 2001.

3.b) 3d-var strategy in ALADIN *(M. Siroka, G. Boloni)*

The results of the family of 3d-var algorithms run last November on LACE domain were examined. To remind, three basic algorithms were tested:

- "STANDARD" using the classical Jb (background term) penalty function and ALADIN +6h forecast as a guess. The same observations are used like in ARPEGE but ATOVS/TOVS, which are not used. There is no Jc (noise control) penalty function in ALADIN.
- "BLENDVAR" using the "mesoscale" Jb penalty function and ALADIN blended state as a guess. Otherwise the rest (observation file and missing Jc penalty function) is like in the STANDARD case. This algorithm is the closest one to the 3d-var multi-incremental approach. The blending step might be considered like the first outer-loop fixing the large-scale part of the spectra consistently with the ARPEGE analysis. The analysis step behind is supposed to analyse something else, hopefully the finer part of spectra. Of course, the long waves might be modified a bit as well but this is true also in the classical multi-incremental approach.
- "VARBLEND" using the "mesoscale" Jb penalty function and ALADIN +6h forecast as a guess. The blending procedure is applied on the result of 3d-var like if the analysis is taken as a guess of the blending. Here the blending step should bring the large scales back to the ARPEGE analysis.

The algorithms were run for couple of days in the assimilation cycles of 6h. Then the results were examined particularly within the forecast window 0-6h in order to see how big are the differences in the first guess of the next analysis step.

The role of the large-scale forcing at the initial time of the forecast

It was noticed that the role of the "0h coupling file" is quite important, especially in the STANDARD case. There were two solutions: i) either to make the lateral boundary and initial conditions identical (the result of the analysis becomes its own lateral boundary forcing at the initial time); ii) or to use the ARPEGE analysis as the lateral boundary condition. Since both BLENDVAR and VARBLEND algorithms fix the long waves according to the ARPEGE analysis, there is not really any noticeable difference between the two solutions. In the STANDARD case the usage of the ARPEGE analysis as the "0h coupling file" was bringing the solution quickly back to the one of BLENDVAR and VARBLEND. The usage of the ALADIN analysis as the "0h coupling file" originated a bit different trajectory (at least up to +6h). Therefore the STANDARD case assimilation cycle was rerun with this option, giving to the STANDARD case the most "independent" algorithm from the ARPEGE assimilation result. On the other hand the fact that the lateral boundary forcing at the initial time dominates the ALADIN trajectory within the first 6 hours of the forecast might be a simple consequence of the relatively small size of the ALADIN/LACE domain.

The balance of the ALADIN analysis and the role of DFI initialization

The STANDARD case analysis was always quite noisy. This result confirmed the experiments of Adam Dziedzic done with the ALADIN/FRANCE configuration in Toulouse. The use of the external initialization is then necessary. On the other hand the BLENDVAR and VARBLEND analyses are already well balanced. The application of the external DFI does not seem to change much the results. Unfortunately, these experiments were not yet run using the incremental DFI technique (where only increments are initialized).

The increments

The shape (broadness) and amplitude of the analysis increments were looked at, also by plotting the charts of differences between the results of the tested algorithms (or between the internal steps within one algorithm). One can say that the increments were rather dependent on Jb: in case of BLENDVAR or VARBLEND with the meso-scale Jb the increments were more "local", sharper, and with smaller amplitude. In the STANDARD case there were large and strong increments, however most of their signal was wiped out like a noise in the following integration.

The spectra

The analysis spectra were examined with the help of "ECTOPLASM" tool. There were not really any big differences between the examined 3d-var algorithms themselves. The "largest" impact on the spectra (taken in the relative sense) was due to the blending step (namely in the wave number interval from 10 to 30). The 3d-var itself was not bringing further change. This result is less encouraging since it could be interpreted as that the ALADIN 3d-var does not analyse more structures than ARPEGE already does (in none of the algorithms). This could be caused by the fact that the ALADIN analysis does not work with denser observation network than the one used by ARPEGE. Perhaps also the Jb term is not really well adapted and tuned.

The scores

Finally the scores of the 6h forecasts (in fact of the guess within the data assimilation cycle) were computed over a short period (against SYNOP and TEMP stations). There were not really any significant differences. Forcing oneself to find the "winner", one could choose the BLENDVAR case.

This first experiment using various 3d-var algorithms brought some interesting results and also it showed us the limits of the current ALADIN 3d-var set-up. At the moment it seems that the STANDARD case does not provide a promising solution if nothing else is done. The most logical and promising is the BLENDVAR case. However, as the whole, the ALADIN 3d-var analysis is not showing much of the performance, in none of the cases.

Unfortunately, the experiment was run at the time when the Prague centre did not have a stable archiving device which limited the storage capacity to be used for these experiments. By consequence, the comparison to the pure blending algorithm (without the use of the observations) could not have been done for that concrete period. Therefore the whole experiment was re-run for another period in May 2001. The results of this period were not yet examined in details. The more recent experiment shall be also completed by the use of the incremental DFI technique. We expect to analyse the results in the second half of 2001 and to provide everybody with a complete report. Before any further important stage of experiments it will be needed to work out better the Jb term or to use significantly more observations than ARPEGE or both.

4. Coupling of surface pressure tendency *(T. Szabo)*

The main development phase of the surface pressure tendency coupling was successfully finished this spring. A major difficulty was to conciliate this method with the semi-implicit treatment of the large-scale forcing. Finally, the solution was to code the tendency coupling as the correction of the "classical" coupling step though this solution also has some weaknesses. The first experiments were done in the 2d vertical plane using the idealized mountain put to the lateral boundary in order to create the difference in orography between the "large-scale" and "high-resolution" model. The new method showed encouraging results. Then one test was done in the full 3d case with ALADIN/LACE. This time one cannot really say which method provided a better result. Perhaps the LACE domain is not the best one for this kind of tests, since the lateral boundary is mostly over sea or flat regions where we cannot expect so significant differences between ARPEGE (large-scale) and ALADIN (fine-scale) orography. A detailed report by Tamas is available in this Newsletter.

5. Spectral coupling *(G. Radnoti)*

This work was motivated by the case of 26 December 1999 storm (denoted as French T1 storm) when the 6h coupling refreshment interval was too long to pass correctly the signal of the fast moving cyclone from ARPEGE to ALADIN/LACE domain. From the experiments done in the beginning of 2000 it is known, that the increased time frequency of the lateral boundary refreshment (to 3h for example) is sufficient to capture the T1 storm by the limited area model. Since this simple solution would be costly in terms of the telecommunications, it is interesting to look for other methods, which could supply the missing time-frequency information. One of this alternative is the so-called spectral coupling, which may provide sufficiently good spatial information (the T1 storm is present in the large scale solution though it passed behind the "coupling belt"; hence it cannot be captured any more by the classical grid-point coupling). The hope is to find a way to combine successfully the grid-point method with the spectral one (the spectral coupling alone cannot be applied). The amplitude-angle-phase method of the spectral coupling was developed and successfully tested in the shallow water model. The difficulties came when generalizing the method to the 3d model. Please, refer to the detailed contribution by Gabor Radnoti in this Newsletter.

6. Horizontal diffusion of humidity *(Thomas Haiden)*

The basic development of this method is finally over, though there remains still one weak conceptual point to be corrected. Despite this point the method seems to work, at least from the point of view of the coherent behaviour, as expected.

To remind the main idea: due to the terrain-following coordinate the diffusion in the model follows the coordinate surfaces, which ceases to be quasi-horizontal in presence of steep orography. Hence the spectral horizontal diffusion operator may create spurious vertical diffusion. In the model a correction exists for the diffusion of temperature, while nothing is done for moisture. The idea tested here consists in making a correction to the moisture convergence fields, assuming that the worse manifestation of the problem lies in the link between dynamics and convective parameterisation.

The method was tested on some pre-selected cases of summer convection in the region of the Alps. The observed effects were rather mild. In order to judge whether the method brings the results closer to the reality, a finer verification will have to be done. It will be necessary to work with radar data (for verification). It will be also useful to verify the assumptions used in the method (the existence of moist bias over the mountains caused by the spurious vertical diffusion of humidity). These two issues are proposed for future work around this subject. A detailed report (written by Thomas Haiden) is available on request.

4. *In Budapest (Hungary)*

INTRODUCTION

In the first half of 2001 efforts were concentrated on the one hand to the filling up of the ALATNET position already advertised in 2000 and on the other hand progress could be identified in the key ALATNET topics for the Hungarian Meteorological Service. From administrative point of view the originally planned post-doc ALATNET stay (after two unsuccessful call for candidates) was converted into a 20 months pre-doc stay in Budapest and finally was filled thanks to the last call of candidates in April (the stay will start in November). Hereafter this short report will concentrate on the main progress on the different scientific topic.

SCIENTIFIC ACTIVITIES

The main scientific achievements will be mentioned with special emphasis on coupling, surface analysis and variational data assimilation (3DVAR).

COUPLING

The started work had been continued in this year as far as surface pressure tendency coupling is concerned. The code developments were completed and tested together with the experimentation of the new scheme (see more details in the same Newsletter).

SURFACE ANALYSIS

The work had been also continued using a new soil texture data base over Hungary. The sensitivity tests carried out this year were concentrated on the CANARI surface analysis scheme based on optimal interpolation. The CANARI scheme was used in data assimilation mode hoping that the accumulated effect of the better surface description will improve the forecasts of the near surface characteristics of the ALADIN model. For the tests some interesting cases were used, when it was expected that significant differences will be found between the experiments using the old and new data sets. The preliminary results show that there are no clear improvements identified using the new data, so further investigations are need in the interpretation of the results.

3DVAR

The main emphasis was put on the background error statistics computed for the ALADIN/HU model version of the ALADIN model. Background error covariance matrices were computed using the NMC method for different integration lengths and integration differences. The aim of the investigations is finding the optimal background errors to be used in the mesoscale data assimilation process for ALADIN. It was shown that longer integration lengths favour the shift of the variance spectra towards larger wavenumbers (smaller scale), however at the same time the energy of the spectra is decreased. It can be seen that an optimal compromise between these two effects should be found for the optimal background error statistics. The investigations should be continued and completed until the end of this year.

SUMMARY

A candidate was successfully found for the ALATNET position in Budapest (stays to be started in November) and reasonable progress can be shown on the ALATNET scientific topics as well. Finally it is remarked that Hungarian colleagues were also working at other different ALADIN centres (mainly in Prague and Toulouse) in the above mentioned topics.

5. In Ljubljana (Slovenia)

The ALATNET actions in Ljubljana or involving the Slovenian team during the first 6 months of 2001 are reported here :

Case studies aspects of NH

Klaus Stadlbacher was concentrating his efforts mainly on finding proper use of orography on high resolution. He was mainly focusing on the methods of removal unrealistic wavy structures in precipitation field. It turned out that the most realistic structures could be obtained with the use of orography on coarser resolution than the other spectral fields. Orography was produced on quadratic grid while the other spectral fields were produced on linear grid, which in fact means an increase of the resolution by a factor of 1.5. For more information see the article of Klaus Stadlbacher in the Proceedings of the ALADIN workshop in Toulouse.

Work of Danijel Cemas in Prague

He was trying to push the limit of high resolution even below 2.5 km what is currently believed the target high resolution. He was able to run the ALADIN model even at 1 km horizontal resolution. The analyses of results has still to be done but the fact that it is able to run the model in such resolution is very encouraging.

Coupling and high resolution modes

Together with Hungarian colleagues the detailed working plan of the new ALATNET student, Raluca Radu from Romania, was produced together with the list of references. Raluca Radu has started her study in Budapest in September.

Deported ALADIN developments during the first half of 2001

1. In Austria

Experiments on MAP cases

To investigate the problems of NWP precipitation forecast over mountainous areas, two ALADIN model simulations with different model resolutions and dynamics were carried out: a) 9.6 km horizontal resolution, hydrostatic; b) 4 km horizontal resolution, non-hydrostatic. The area of the investigation is the Ticino (CH), which is well documented in MAP (Mesoscale Alpine Programme) and the EU-Project RAPHAEL. The cases studied so far are MAP IOP2 (19 Sep 1999 00Z - 22 Sep 1999 00Z) and IOP3 IOP2 (25 Sep 1999 00Z - 28 Sep 1999 00Z). Model results are compared to radar data. Both the lower and higher resolution ALADIN forecasts overestimate the amount of precipitation on the southern slopes, with the 4km simulation overestimating it more strongly. At the northern side the forecasts appear too dry, i.e. the upwind/downwind precipitation contrast is too pronounced in the model. At 4 km resolution, the explicit part of the precipitation is much larger than at 9.6 km, as expected. The model was also run in quasi-diagnostic mode (just 1 time-step, starting from analysis) and the resulting precipitation rates compared to the standard run. Precipitation was generally less, purely convective (in disagreement with observations), and not closer to reality. It could be that the analysed humidity field over the mountains is too dry, but this needs to be further investigated. [For further details contact Yong Wang]

Mountain convection

A three-day period of daytime convective precipitation triggered by mesoscale processes in Alpine terrain is studied using ALADIN (AL11, AL12). The period chosen is characterized by light westerly flow across the Alps, with no major front or other synoptic disturbance affecting the area. Modelled convective rainfall is compared with radar data. Moist static energy is used as a diagnostic quantity to investigate the role of PBL temperature and moisture in determining where convection is initiated. It was found that the locations of convective activity can be largely explained by the PBL moisture distribution, and individual topographic features. A significant asymmetry in the PBL wind and moisture field with regard to the upwind and downwind sides of the Alpine barrier is found. Generally, the model shows significant skill in predicting initiation sites of mountain convection. With regard to timing the model tends to start convection too early by several hours. This could be a result of an overestimation of PBL moisture levels, which was found on all three days. A summary of results from Day 1 of the period will appear in Haiden (2001). [For further details contact Thomas Haiden and Stefan Greilberger]

ACuVis

A comprehensive visualization system (**A**LADIN **Cu**stomized **Vis**ualization) for operational use of ALADIN-VIENNA forecast fields has been developed. The system, which has been programmed in VisualC, runs on PC platforms. It allows fast and easy visual access to 3d and 2d ALADIN forecast fields. In addition to horizontal maps with various overlays such as topography or the river system, user-defined vertical slices and model soundings can be obtained by mouseclick for any point within the map. Horizontal maps, vertical slices, and soundings can all be run in time-loop mode. Interpolation between the model output times (interval 1 hr) creates smooth field evolutions even at low loop speeds. A special binary data format containing header information for the visualization has been created. After a pre-operational test period of 1-2 months ACuVis will be used beginning this fall at the forecast center in Vienna and at the regional services. [For further details contact Fabian Haiden (fhaiden@q3arena.com) and Thomas Haiden]

ALADIN **Cu**stomized **Vis**ualization for operational use of ALADIN-VIENNA forecast fields has been developed. The system, which has been programmed in VisualC, runs on PC platforms. It allows fast and easy visual access to 3d and 2d ALADIN forecast fields. In addition to horizontal maps with various overlays such as topography or the river system, user-defined vertical slices and model soundings can be obtained by mouseclick for any point within the map. Horizontal maps, vertical slices, and soundings can all be run in time-loop mode. Interpolation between the model output times (interval 1 hr) creates smooth field evolutions even at low loop speeds. A special binary data format containing header information for the visualization has been created. After a pre-operational test period of 1-2 months ACuVis will be used beginning this fall at the forecast center in Vienna and at the regional services. [For further details contact Fabian Haiden (fhaiden@q3arena.com) and Thomas Haiden] for operational use of ALADIN-VIENNA forecast fields has been developed. The system, which has been programmed in VisualC, runs on PC platforms. It allows fast and easy visual access to 3d and 2d ALADIN forecast fields. In addition to horizontal maps with various overlays such as topography or the river system, user-defined vertical slices and model soundings can be obtained by mouseclick for any point within the map. Horizontal maps, vertical slices, and soundings can all be run in time-loop mode. Interpolation between the model output times (interval 1 hr) creates smooth field evolutions even at low loop speeds. A special binary data format containing header information for the visualization has been created. After a pre-operational test period of 1-2 months ACuVis will be used beginning this fall at the forecast center in Vienna and at the regional services. [For further details contact Fabian Haiden (fhaiden@q3arena.com) and Thomas Haiden] special binary data format containing header information for the visualization has been created. After a pre-operational test period of 1-2 months ACuVis will be used beginning this fall at the forecast center in Vienna and at the regional services. [For further details contact Fabian Haiden (fhaiden@q3arena.com) and Thomas Haiden]. After a pre-operational test period of 1-2 months ACuVis will be used beginning this fall at the forecast center in Vienna and at the regional services. [For further details contact Fabian Haiden (fhaiden@q3arena.com) and Thomas Haiden] ACuVis will be used beginning this fall at the forecast center in Vienna and at the regional services. [For further details contact Fabian Haiden (fhaiden@q3arena.com) and Thomas Haiden]

<u>See also :</u>
"*Orographically triggered convection : a case study*", by Thomas Haiden, in the proceedings of the 10th ALADIN workshop.

2. *In Belgium*

Installation and test of a CANARI assimilation suit for ALADIN/Belgium.

<u>Preparing the ALATNET training course on data assimilation</u>

topic : Blending (case studies)

<u>See also :</u>
"*Tests of some temporal interpolation schemes for the coupling mechanism*", by Piet Termonia, "*Some results using a prognostic convection scheme in ARPEGE-ALADIN*", by Luc Gérard, in the proceedings of the 10th ALADIN workshop, and the ALATNET reports.

3. *In Bulgaria*

The visualization for predicted rainfall totals and snow quantity was changed : shaded plot was used for the intervals: 1, 5, 10, 15, 20, 30, 50, 80 and more then 80 mm. Either the shade area was bordered by isolines with plotted values. Following the request of forecasters, on every map of forecasted field eight Bulgarian cities are marked with circles. On the figure below is shown an example of new design. Since third quarter of 2000 the graphical output of ALADIN-BG forecast is accessible for our regional branches.

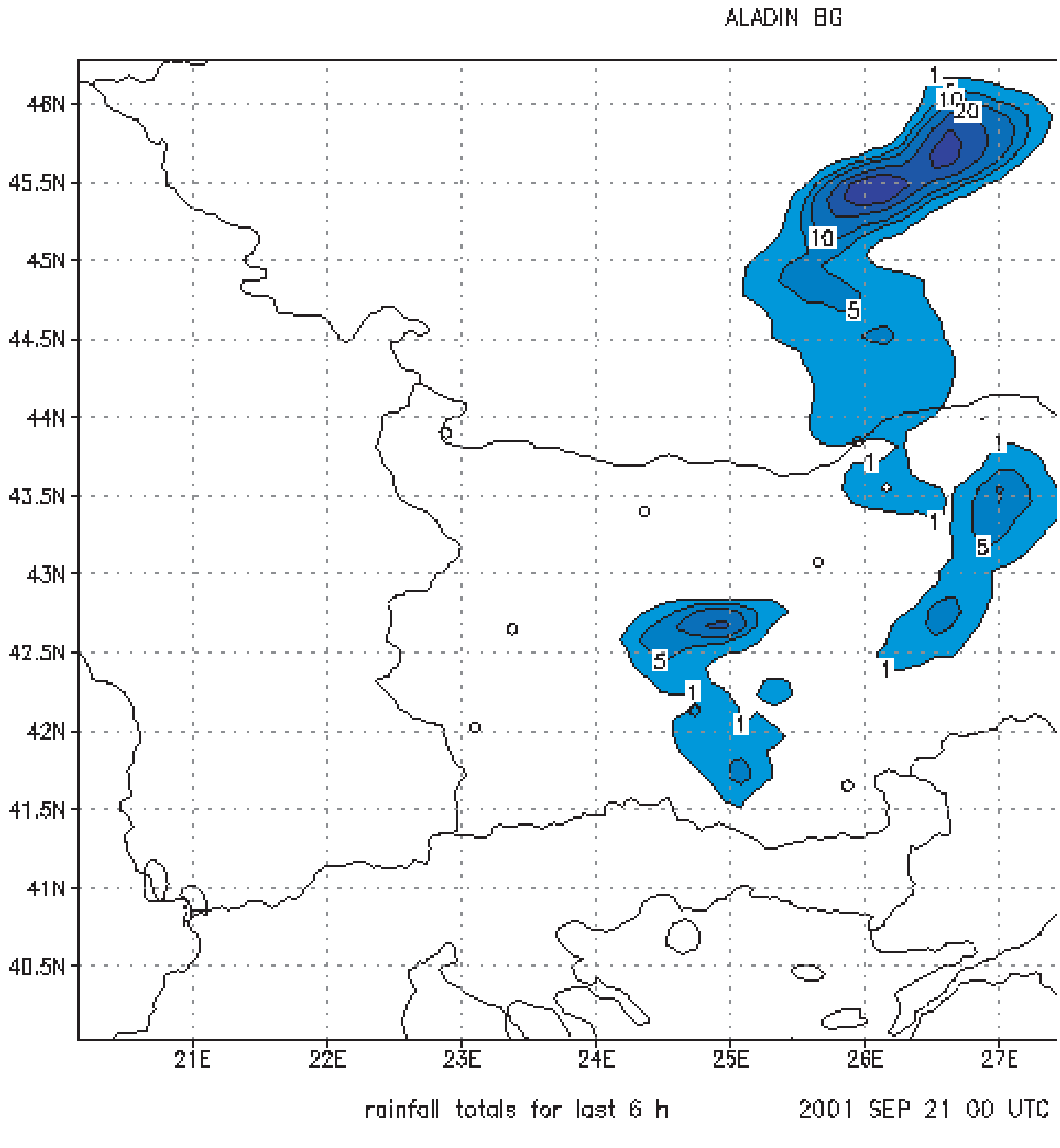

New verification scheme for surface elements was introduced since February of 2001. We use as initial conditions 12h forecast of ARPEGE. That's why for us it is important to verify the ALADIN-BG forecast against the analyses. This explains the presence of estimation for 00 H forecast in verification scores. Verified elements were : 2m temperature, wind speed and direction at 10m, 2m relative humidity and mean-sea-level pressure. For all elements, except the wind direction was calculated the following scores ME - bias, MAE - mean absolute error. For the wind speed the geographical directions were divided in eight categories and was calculated the percentage of points with wind direction in the same category, the next category and other.

Table 1. Verification scores for 2m temperature. April 2001

H	ME	MAE	RMSE
00	-0.464	0.854	1.136
12	0.465	1.008	1.423
24	-0.694	1.296	1.764
36	0.550	1.313	1.832
48	-0.649	1.420	1.891

Table 2. Verification scores for 10m-wind velocity. April 2001

H	ME	MAE	RMSE
00	0.108	0.499	0,789
12	0.602	1,029	1,397
24	0.585	1,067	1,491
36.	0.543	1,176	1,590
48	0.478	1,160	1,570

Table 3. Verification scores for 2m relative humidity. April 2001

H	ME	MAE	RMSE
00	-1,8	4,1	5,6
12	-9,9	12,5	15,8
24	-7,2	9,4	12,8
36	-10,9	14,2	17,9
48	-7,8	10,5	14,2

Table 4. Verification scores for mean-sea-level pressure. April 2001

H	ME	MAE	RMSE
00	-0,872	0,975	1,240
12	-0,235	1,001	1,287
24	-0,527	1,253	1,583
36	-0,087	1,484	2,009
48	0,415	1,572	2,228

Table 5. Verification scores for 10m-wind direction. April 2001

H	Same	Next	Other
00	83,9	14,8	1,3
12	72,6	24,9	2,5
24	69,2	26,8	4,1
36	65,4	29,3	5,3
48	60,4	30,7	8,9

The units for the elements are as follows: temperature - K, wind velocity - m/s, relative humidity - %, MSL pressure - hPa, and wind direction - %. All computations were made for model grid points.

A new statistical adaptation scheme has been developed. It is used for interpolation over an orography with finer resolution than the one used in ALADIN-BG or for interpolation to an arbitrary point, respecting the real orography characteristics at this point. This scheme is applicable to orography dependent fields, mainly for the temperature at 2 meters and at the surface. The scheme will be verified using records from automatic stations soon placed in mountain areas. The new scheme will be compared with the forecasted temperature at the closest grid point and with the value obtained by bilinear interpolation

4. In Croatia

<u>See also :</u>
"*ALADIN/CROATIA : One year experience on PC-Cluster*", by Dijana Klaric, in the proceedings of the 10th ALADIN workshop.

5. In Czech Republic

<u>Preparing the ALATNET training course on data assimilation</u>

topic : Blending (case studies)

<u>See also</u> the ALATNET reports.

6. In Hungary

<u>Activities around the workstation version of ALADIN</u>

During the last half year the following main activities were performed around the workstation version of ALADIN:

-- The operational model version is still AL12 however in this period AL13 was installed and probably will be used for the ongoing research and development work (ALATNET). The new surface pressure tendency coupling was coded into that cycle (report of this work is available from Tamas Szabo) as well.

-- The work related to the introduction of new soil texture data into the surface characteristcis of the model had been continued having data assimilation experiments (using CANARI). The results so far doesn't clearly show any significant forecast improvements due to the consideration of more precise local soil data (this work served as a basis for the Master work of Agnes Mika).

-- The work related to the lagged NMC method had been continued too. Sensitivity of the lagged formulation was demonstrated with respect to the forecast lengths and forecast differences used in the algorithm (this work was presented in the last ALADIN workshop and going to appear in the proceedings of that workshop, it is also mentioned that this work forms the Master work of Gergely Boloni).

-- The Kalman-filter algorithm was successfully implemented for the bias-correction of the 2m temperature forecasts of the ALADIN/HU model (this work was also presented as a Master work).

-- Test runs of the ALADIN model on a SUN Ultra Enterprise 10 000 system having 96 UltraSparc 250 MHz processors. The tests showed that these SUN processors are relatively slow (one processor is around 1,5 times slower than an Origin 2000 400 MHz processor), however the scalability of the system is pretty good.

<u>Preparing the ALATNET training course on data assimilation</u>

topics : Variational, DiagPack

<u>See also :</u>

"*Lagged constant coupling background error statistics : preliminary results for the ALADIN /HU model*", by Andras Horanyi and Gergely Bölöni, in the proceedings of the 10th ALADIN workshop, the articles and the ALATNET reports.

7. In Moldavia

- Nothing reported.

8. In Morocco

Preparing the ALATNET training course on data assimilation

topics : Variational, Observations

9. In Poland

See also :
"*Last developments of ALADIN operational environment at IMWM*", by Marek Jerczynski, in the proceedings of the 10th ALADIN workshop.

10. Portugal

Tests are being done in order to introduce operationally version AL12_bf02 (CYCORA-bis). A parallel suite has been run during one and a half month so the objective verification procedures will tell us about this possibility.

The configuration e923 is being tested to version AL12_bf02 as well as a new domain for the ALADIN/Portugal area domain in order to reduce resolution to 10 km.

On the analysis/assimilation field, a scheme for producing CMAFOC files from the Portuguese Meteorological DataBase (PMDB), where observational data is in BUFR format, has been installed, using local developed interfaces, and the packages OULAN and MANDALAY. Moreover, the installation of both CANARI (AL13) and CANARI (AL11) are being tested, the first for diagnostic purposes, using DIAGPACK and the second for assimilation purposes.

Finally, diagnostic tools for severe weather events over Portugal using ALADIN forecasts are being developed and tested.

11. In Romania

See also : "*Tuning the orography representation in the E923 configuration*" by Steluta Alexandru, "*Simulation of the meso-scale convective systems at different resolutions*" by Doina Banciu, "*Some applications of the ALADIN model in Romania*" by Mihaela Caian, in the proceedings of the 10th ALADIN workshop.

12. In Slovakia

Preparing the ALATNET training course on data assimilation

topic : Structure functions

13. In Slovenia

Preparing the ALATNET training course on data assimilation

topic : DiagPack

See also :

"*Implementation of CAPE and CIN in ALADIN* " by Neva Pristov and Jean-Marcel Piriou, in the proceedings of the 10th ALADIN workshop, and the ALATNET reports.

14. In Tunisia

Tunisia has just joined the project this semester.

15. Deported work by Météo-France people

Nothing this semester.

ALADIN developments in Prague during the first half of 2001

Note: all ALATNET related R & D, representing the majority of the effort, is reported in ALATNET Newsletter. Here we sum-up topics which are not referred as ALATNET ones for Prague centre.

1. Developments in physics

- *Diagnostics of PBL height*

Though the first version of PBL height diagnostics is already produced operationally, this product is not yet really ripe and it still needs further refinements. As implemented in the cycle AL12_op6, it quite often happens that the resulting PBL height is either too small (below 1 meter or even very close to zero) or too high (even above 8km). The behaviour of the current scheme was extensively tested in ALADIN/LACE. The problems occur especially over hills and valleys and above the sea surface (too low values of PBL height) or under specific conditions like deep temperature inversions, very strong wind (too high values of PBL height). The diurnal evolution of PBL height is quite visible. The diagnostic scheme was modified and tested in order to avoid too small PBL heights. The modification improves the results, but it does not solve yet other weaknesses. There is a detailed report (written by

Martina Tudor) available in Prague on request. The report describes well the current scheme and tests of it made with ALADIN/LACE, as well as the proposed modification.

More details can be asked to: Martina Tudor and Jean-François Geleyn.

- Diagnostic of winter PBL moisture

It was noticed by the forecasters that the model over-dries the PBL at the lee side of the mountains in winter. Therefore the diagnostic of this feature was done using ALADIN/LACE on some pre-selected typical cases from February 2001. The over-drying was confirmed, however the reason is not yet understood. The bias in relative humidity is quite important (reaching up to 35% at some SYNOP stations) in the region of North-East Austria. On the other hand the temperature and wind forecast were quite good. One plausible explanation was checked: whether there is not a kind of Tanguay-Ritchie effect concerning the physical forcing (in analogy with the orographic forcing). Therefore the experiment was rerun in the Eulerian mode but without a real change of the humidity forecast. Another test consisted in suppressing the horizontal diffusion of humidity to avoid fictitious vertical diffusion of humidity along the mountain slopes (there actually was a layer of quite a dry air above as confirmed by Vienna sounding) but again without any significant effect on the humidity forecast. The preliminary conclusion is that one has to look closer to the PBL parameterization in order to understand more the mechanism of the dry air intrusion into the surface layer.

More details can be asked to: Harald Seidl, Thomas Haiden, Filip Vana.

2. *Developments in the verification*

- Verification of precipitation

The tool VERAL is going to be extended in order to compute the scores of precipitation. This has been a long time goal of RC LACE. There were many technical problems, related especially to the correct representation of the precipitation amounts in the observation CMA-format files, both regarding the quantity compared to the model forecasts and the interval of measurements. The updated VERAL should be at disposal in a near future.

RC LACE Management Group discussed the verification strategy in general. Thanks to the stabilized archive in Prague, it becomes possible to compute the ALADIN/LACE scores systematically and to work out the basic scores in a continuous manner. A list of scores to be produced was discussed and established.

More details can be asked to: Dijana Klaric, Zuzana Huthova.

3. *Technical developments*

- Configuration E923

The configuration for computing the climatological boundary constants was finally ported to the NEC SX4 platform. Most of the problems were linked to the different representation length of INTEGER numbers in the datasets and on the machine. The E923 configuration was also ported to the LINUX server voodoo. This configuration is important in order to prepare the tests of ALADIN on a 1 km horizontal mesh having a correct representation of the orography.

More details can be asked to: Jure Jerman

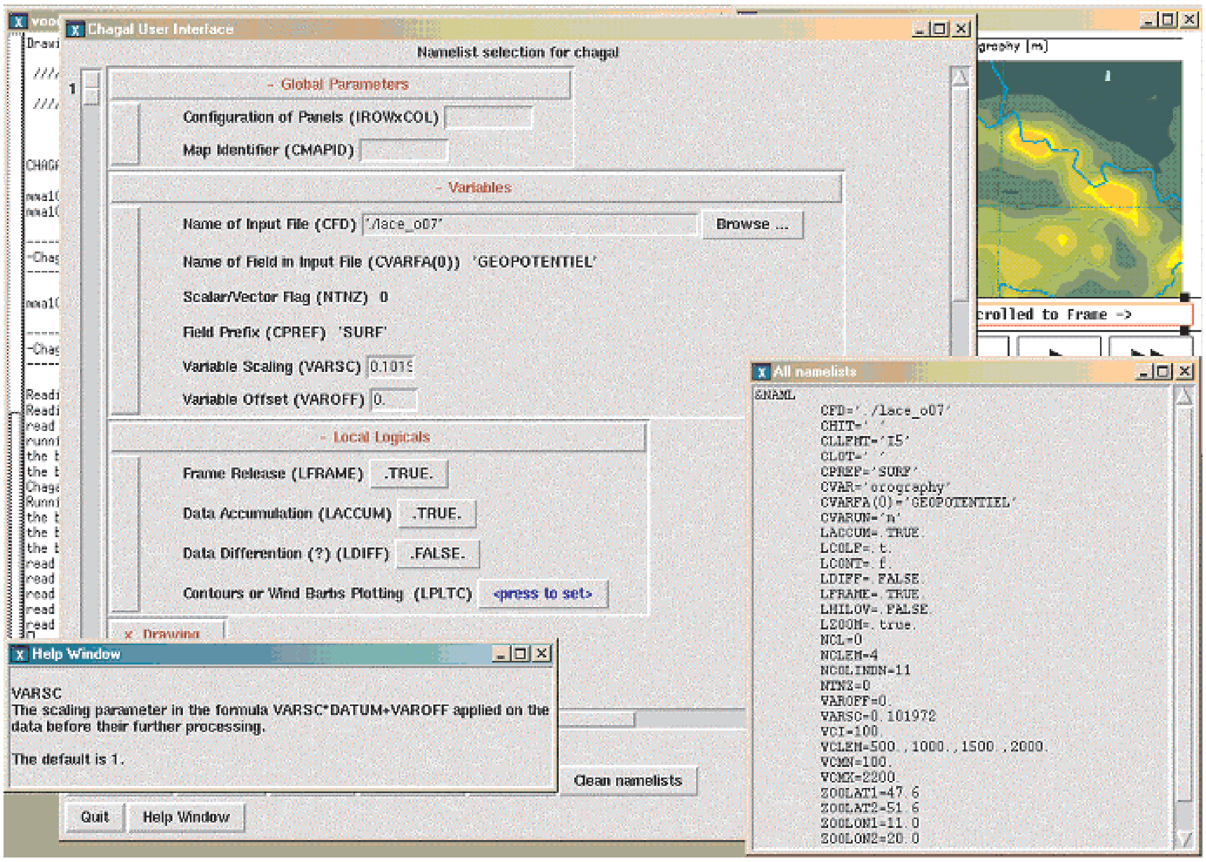

- CHAGAL User Interface

The development of the Tk-based user interface to CHAGAL namelist has progressed. Its author, Tomas Kalibera, ported it to LINUX platform and made its extensive tests. The tool is designed to support a quick creation of new CHAGAL namelists and their modification as well as to launch CHAGAL program for easy visualization of the horizontal fields in ALADIN files.

Some minor changes and improvements have been made also in the CHAGAL itself to meet needs of the local ALADIN development team.

More details: Tomas Kalibera, Martin Janousek

ALADIN developments in Toulouse during the first half of 2001

The new ALADIN library, AL15, is now ready, thanks to the self-sacrifice of Claude Fischer and the help from a few brave ALADINers : Lora Gaytandjieva, Stjepan Ivatek-Sahdan, Martin Janousek, Jan Masek, Gabor Radnoti, Vanda Sousa da Costa, Malgorzata Szczech, and Ryad El Khatib. However some more work is still required, especially concerning observation handling, optimization, e923, ...

Karim Bergaoui, Nihed Bouzouita and Abdelwaheb Nmiri prepared the new ALADIN-Tunisie suite, with some help from Jean-Marc Audoin and Jean-Daniel Gril : benchmark and definition of the pre-operational version to be temporarily run in Toulouse. Part of their stays was also devoted to further training.

Blazenka Vukelic prepared the "EUROCS Stratocumulus Case" observational dataset for use in the 1d version of ARPEGE/ALADIN. The first experiments showed that the current physics is not as bad as foreseen, and identified two major deficiencies in such situations : too much intermittency due to spurious triggering of the "deep convection" scheme, and a significant underestimation of cloudiness within the "vertical diffusion" scheme.

The first problem was also mentioned by Frédéric Sourgen, who studied the respective impacts of physics and resolution on the forecast of the tropical cyclone FLO by ALADIN. He also analysed the behaviour of the convection scheme as the resolution decreases (from 50 to 5 km), and exhibited a strong underestimation of evaporation over sea. The second problem was addressed by Janko Merse. Some more details on these two studies are given in the ALATNET report.

Jean-Marcel Piriou improved the partition of convective (unresolved) precipitations between solid and liquid ones, so as to avoid snowfalls in warm air as it sometimes happened on rather colder soils. The temperature above the current vertical level is now considered (instead of the local temperature), as was already the case for stratiform (resolved) precipitations.

A new tool was designed to simulate "infra-red" or "water vapour" brightness temperatures from model fields, for diagnostic or validation purposes. Different radiation schemes may be used. For more details, contact : *Jean-Marcel.Piriou@meteo.fr*.

After several months of test and retuning, involving François Bouyssel and Françoise Taillefer, Diag-Pack is now pre-operational at Météo-France. Hourly analyses, based on ALADIN-France and all available SYNOP-type observations, are sent to three regional centres for real-time validation.

To end with, the Toulouse team provided many teachers to the ALATNET training course, and also an efficient organisation team : Patricia Pottier and Jean-Daniel Gril.

Contents